https://doi.org/10.1016/j.jpowsour.2016.08.105

Recent progress in alkaline direct ethylene glycol fuel cells for sustainable energy production

L. An[a]* and R. Chen[b,c]*

[a] Department of Mechanical Engineering, The Hong Kong Polytechnic University, Hung Hom, Kowloon, Hong Kong SAR, China

[b] Key Laboratory of Low-grade Energy Utilization Technologies and Systems (Chongqing University), Ministry of Education, Chongqing 400030, China

[c] Institute of Engineering Thermophysics, Chongqing University, Chongqing 400030, China

*Corresponding authors.

[a] Tel.: 852-27667820; fax: 852-23654703; e-mail: liang.an@polyu.edu.hk (L. An)

[b,c] Tel.: 86-23-65102474; fax: 86-23-65102474; e-mail: rchen@cqu.edu.cn (R. Chen)

Abstract

Alkaline direct ethylene glycol fuel cells are one of the most promising power sources for portable, mobile and stationary power applications, primarily because this type of fuel cell runs on a sustainable fuel and the key materials that constitute the fuel cell are relatively inexpensive. This review article summarizes and discusses the past investigations on the development of alkaline direct ethylene glycol fuel cells, including the physical and chemical processes through the fuel cell structure, the electrocatalytic oxidation and electrocatalysts of ethylene glycol, the singe-cell performance, and innovative system designs.

Keywords: Fuel cells; Ethylene glycol; Direct ethylene glycol fuel cells; Electrocatalytic oxidation; Electrocatalysts; System designs

1. Introduction

In response to the escalating energy crisis and related pollution problems, we must adopt new energy supply technologies that utilize renewable energy sources in an efficient and environmentally friendly manner. Alkaline direct oxidation fuel cells (DOFC) running on various liquid fuels promise to be a sustainable energy technology, mainly due to the improved performance as a result of fast electrochemical kinetics on both the anode and cathode in alkaline media [1-5]. Among various liquid fuels, ethanol has been recognized as the most suitable fuel as it is a sustainable and carbon-neutral transportation fuel [6-10]. However, a critical issue associated with an alkaline DOFC running on ethanol (DEFC) is that with state-of-the-art electrocatalysts, it is extremely difficult to break the C-C bond in ethanol at temperatures lower than 100^{o}C, and thus the main product of ethanol oxidation reaction (EOR) is acetate [11, 12]. Hence, the actual and theoretical electron transfer numbers per one ethanol molecule are 4 (partial oxidation of ethanol to acetic acid) and 12 (complete oxidation of ethanol to carbon dioxide), respectively. As such, the electron transfer rate (ETR) of ethanol in the alkaline DOFC is only 33%, much lowering the Faraday efficiency. For this reason, finding alternative liquid fuels with a high ETR to replace ethanol becomes essential. Ethylene glycol (EG) is another choice for alkaline DOFCs, because the main product of the ethylene glycol oxidation could be oxalate [13, 14] such that the ETR reaches 80%, which is much higher than that in the alkaline DEFC. Also, ethylene glycol is much less volatile due to the high boiling point (198^{o}C) [15]. In addition, ethylene glycol has the potential to be an energy carrier in an energy-storage system, since ethylene glycol can be synthesized via an electrochemical approach using renewable energy [21, 22]. For these reasons, alkaline DOFCs running on ethylene glycol (DEGFC) have recently received ever-increasing attention and a great progress has been made to this type of fuel cell [16-20]. The objective of this review article is to summarize recent advances and developments on alkaline direct ethylene glycol fuel cells.

2. General description

A typical alkaline DEGFC setup consists of a membrane electrode assembly (MEA) sandwiched between an anode and a cathode flow field. The MEA is composed sequentially of an anode diffusion layer (DL), an anode catalyst layer (CL), an anion exchange membrane (AEM), a cathode CL, and a cathode DL. On the anode, the fuel solution feeding into the anode flow field is transported through the anode DL to the anode CL, where ethylene glycol oxidation reaction takes place to theoretically produce electrons, water and carbon dioxide according to:

$$HOCH_2-CH_2OH+10OH^- \rightarrow 2CO_2+8H_2O+10e^- \qquad \mathrm{E_a^o}=-0.81\mathrm{V} \qquad (1)$$

As mentioned earlier, the main product of the ethylene glycol oxidation reaction could be oxalate. Under this circumstance, ethylene glycol is partially oxidized to produce electrons, water and oxalate according to:

$$HOCH_2 - CH_2OH + 10OH^- \rightarrow (COO^-)_2 + 8H_2O + 8e^- \qquad \mathrm{E_a^o} = -0.69\mathrm{V} \quad (2)$$

On the cathode, the oxygen/air is transported to the cathode CL, where the oxygen reduction reaction (ORR) occurs according to:

$$O_2 + 4H_2O + 4e^- \rightarrow 4OH^- \qquad \mathrm{E_c^o} = 0.40\mathrm{V} \quad (3)$$

The generated hydroxide ions migrate through the membrane to the anode for the ethylene glycol oxidation reaction. Combining the ethylene glycol oxidation reaction given by Eq. (1) or Eq. (2) and the ORR given by Eq. (4) results in an overall reaction:

$$HOCH_2 - CH_2OH + {}^5\!/_2\, O_2 \rightarrow 2CO_2 + 3H_2O \qquad \mathrm{E^o} = 1.21\mathrm{V} \quad (4)$$

or

$$HOCH_2 - CH_2OH + 2O_2 + 2OH^- \rightarrow (COO^-)_2 + 4H_2O \qquad \mathrm{E^o} = 1.09\mathrm{V} \quad (5)$$

In the following sections, we discuss the electrocatalytic oxidation and electrocatalysts of ethylene glycol, singe-cell performance, as well as innovative system designs.

3. Electrocatalytic oxidation and electrocatalysts of ethylene glycol

3.1. Electrocatalytic oxidation of ethylene glycol

The electrocatalytic oxidation of ethylene glycol in alkaline media is a complex reaction due to the presence of several adsorbed intermediates and reaction products/by-products, which could poison the electrocatalysts. Hence, better understandings on the mechanism of ethylene glycol oxidation on a certain electrode will definitely promote the development of the high-activity and high-selectivity electrocatalysts toward the electrocatalytic oxidation of ethylene glycol. Over the past decades, the electrocatalytic oxidation of ethylene glycol on various metal electrodes in alkaline media has been extensively investigated, such as platinum (Pt) [23-38], palladium (Pd) [24, 39-45] and gold (Au) [28, 31, 46-48].

3.1.1. Platinum

Pt or Pt-based electrodes for the electrocatalytic oxidation of ethylene glycol in alkaline media have been extensively investigated [23-38]. Bayer et al. [23] studied the electrocatalytic oxidation of ethanol and ethylene glycol on a polycrystalline Pt foil electrode in acid and alkaline media via cyclic voltammetry, chronoamperometry and differential electrochemical mass spectrometry. It was shown that in alkaline media, the current densities of ethylene glycol oxidation obtained in cyclic voltammetry and chronoamperometry were substantially higher than that achieved by the ethanol oxidation, indicating that as compared to ethanol, ethylene glycol was easier to be oxidized and showed less poisoning effect on Pt in alkaline media. Xie et al. [24] compared the electro-oxidation of various alcohols on Pt and Pd electrodes via a three-electrode cell, including methanol, ethanol, n-propanol, isopropanol, ethylene glycol and glycerol. They found that the electro-oxidation of ethylene glycol and glycerol showed the best electrocatalytic activity on the Pt electrode. Matsuoka et al. [25] investigated the electrocatalytic oxidation of polyhydric alcohols, including ethylene glycol, glycerol, meso-erythoritol, and xylitol, on a Pt electrode in H_2SO_4, KOH, and K_2CO_3 solutions. It was shown that the electro-oxidation of all polyhydric alcohols exhibited high activities in KOH and K_2CO_3 solutions, among which the electro-oxidation of ethylene glycol showed the highest electrocatalytic activity. In addition, it was also shown that EG encountered much less electrocatalyst poisoning by the adsorbed CO species in alkaline media. Matsuoka et al. [26] proposed the mechanism for electrocatalytic oxidation of ethylene glycol on the Pt surface in alkaline media. They suggested that there were two pathways for the electrocatalytic oxidation of ethylene glycol, i.e., poisoning and non-poisoning pathways, as illustrated in Fig. 1a. It can be seen that ethylene glycol could be oxidized to oxalate via a non-poisoning pathway or to formate via a poisoning pathway. The poisoning pathway means further oxidation of formate will produce CO poisoning species; but for non-poisoning pathway, oxalate is stable in alkaline media and difficult to be further oxidized such that there will be no poisoning species formed on the Pt surface.

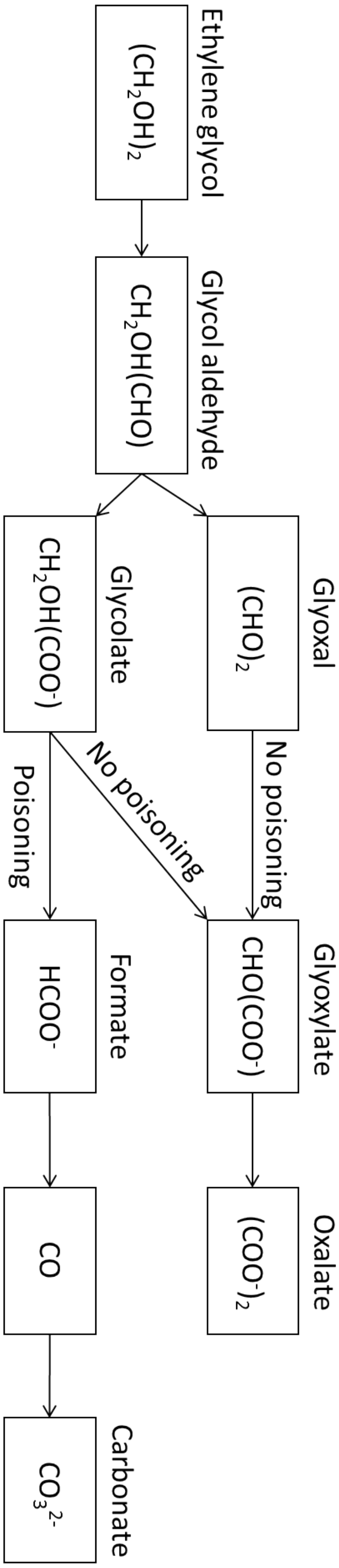
Ethylene glycol
$(CH_2OH)_2$
Glycol aldehyde
$CH_2OH(CHO)$
Glyoxal
$(CHO)_2$
Glycolate
$CH_2OH(COO^-)$
No poisoning
No poisoning
Poisoning
Glyoxylate
$CHO(COO^-)$
Formate
$HCOO^-$
Oxalate
$(COO^-)_2$
CO
Carbonate
CO_3^{2-}

(a)

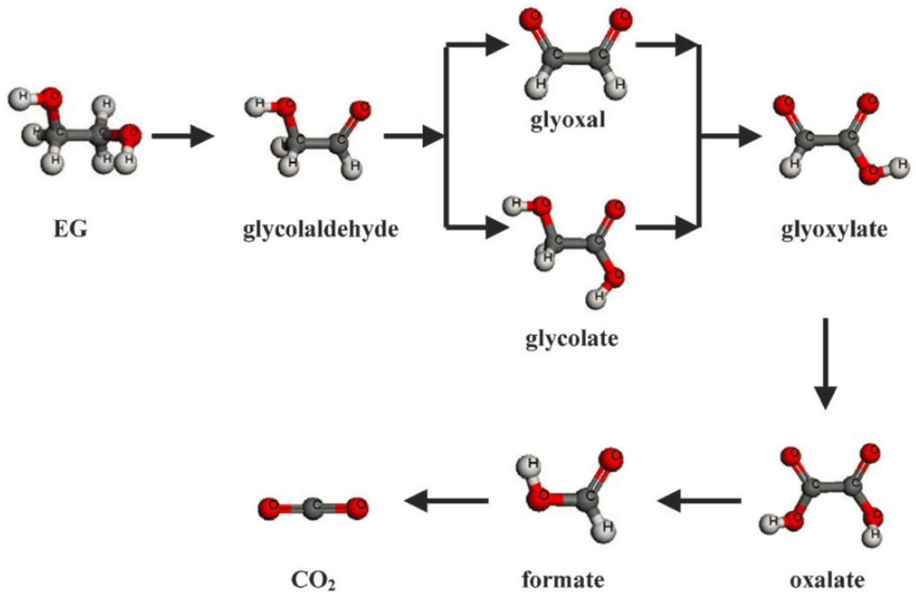

(b)

Fig. 1 (a) Reaction pathways of ethylene glycol electro-oxidation in alkaline media [26]. Reproduced with permission from Elsevier. (b) Reaction pathway of ethylene glycol electro-oxidation on a Pd electrode in alkaline media [40]. Reproduced with permission from The Royal Society of Chemistry.

It can be seen from the proposed mechanism that many C_2 intermediates/products/by-products could be produced in the electrocatalytic oxidation of ethylene glycol on Pt, mainly including glycol aldehyde, glyoxal, glycolate glyoxylate, oxalate and formate. Christensen et al. [27] examined the products of the ethylene glycol oxidation on a Pt electrode in acid and alkaline media via in-situ FTIR spectroscopy. It was found that in alkaline media, the main products were glycolate, oxalate and carbonate, among which glycolate and carbonate were produced from the same intermediate; while, oxalate was produced from further oxidation of desorbed glycolate. In addition, the poisoning effect also occurred in alkaline media, but the poisoning species was not specified. Chang et al. [28] studied the electrocatalytic oxidation of ethylene glycol on Pt in alkaline media via real-time FTIR spectroscopy and cyclic voltammetry. They pointed out that carbonate was produced from chemisorbed intermediates rather than solution-phase intermediates. Hahn et al. [29] investigated the adsorption of ethylene glycol on a Pt electrode via electrochemically modulated infrared reflectance spectroscopy. It was shown that the adsorption appeared to be dissociative at pH ranging from 1 to 13, and striking changes in the composition of the adsorbed layer occurred when the pH was higher than 7. In addition, it was suggested that linearly bonded CO was dominated at pH ~ 1; while, almost equal amounts of bridge-bonded and linearly bonded CO species were found at pH ~ 13. Sitta et al. [30] investigated the effect of alkali cations on the electrocatalytic oxidation of ethylene glycol on a Pt electrode in alkaline media via in-situ IR spectroscopy. It was found that the interaction between adsorbed oxygenated species and alkali cations strongly affected the electro-oxidation of ethylene glycol on polycrystalline Pt. It was also found that an increase in the anodic current ($Li^+ < Na^+ < K^+$) was attributed to the increased cleavage of the C-C bond. Angelucci et al. [31] studied the effect of cations on the electrocatalytic oxidation of ethylene glycol and glycerol on Pt and Au in alkaline media via cyclic voltammetry and chronoamperometry. They showed that the reaction was affected by OH_{ad}-$M^+(H_2O)_x$ clusters from non-covalent interactions between hydrated alkali cations ($M^+(H_2O)_x$, $M^+ = Li^+$, Na^+ and K^+) and OH_{ad}. Sitta et al. [32] studied the potential oscillations during the electrocatalytic oxidation of ethylene glycol on Pt in alkaline media. It was observed that the oscillation frequencies reached as high as 16.8 Hz. They pointed out that those potential oscillations were the fastest among small organic molecules. In addition, the oscillations were also observed at different temperatures and rather insensitive to the temperature. Sitta et al. [33] further investigated the electrocatalytic oxidation of ethylene glycol on polycrystalline Pt surfaces in alkaline media with the consideration of the effects of experimental parameters (applied current, ethylene glycol concentration and temperature) on the oscillatory dynamics, via electrochemical impedance spectroscopy, cyclic voltammetry, and chronoamperometry. It was again observed that the oscillation frequencies reached about 16 Hz. In addition, those high frequencies were strongly affected by the pH of the electrolyte.

It has been shown that the use of different metals alloyed with Pt is the simplest strategy to improve the activity of the ethylene glycol oxidation due to synergistic effects in electrocatalysis. Hence, the ethylene glycol oxidation on Pt-M electrocatalysts has been extensively studied [34-36]. Matsuoka et al. [34]

investigated the electrocatalytic oxidation of ethylene glycol on Pt-based electrocatalysts, i.e., Pt-Ru/C and Pt-Pb/C, and Au/α-Fe_2O_3/Pt/C in alkaline media. It was found that the electrocatalytic activity was enhanced with Pt-Ru/C, PtPb/C and Au/α-Fe_2O_3/Pt/C as compared to Pt/C. In addition, it was also suggested that Au suppressed CO poisoning as a result of the fact that Au showed the highest electrocatalytic activity toward the ethylene glycol oxidation in potentials lower than 200 mV. Demarconnay et al. [35] studied the electro-oxidation of ethylene glycol on Pt-based electrocatalysts in alkaline media. It was found that the addition of Bi to Pt decreased the onset potential of ethylene glycol oxidation by about 70 mV and resulted in higher current densities. They explained that the enhancement of the electrocatalytic activity in the presence of Bi was attributed to the bi-functional theory of electrocatalysis; while an addition of Pd alleviated the poisoning effect [36]. They further prepared the ternary Pt-Pd-Bi/C electrocatalysts and found that they did not change the onset potential, but increased the current densities as compared to the binary Pt-Bi electrocatalysts.

In addition, the modification of the electrode surface is able to further improve the electrocatalytic activity by foreign metal ad-atoms. Hence, the activity of the ethylene glycol oxidation on foreign metal ad-atoms modified Pt electrodes has been extensively studied [37, 38]. Kadirgan et al. [37] studied seven different foreign metal ad-atoms (Bi, Cd, Cu, Pb, Re, Ru, Tl) as modifiers on Pt electrodes for the ethylene glycol oxidation in alkaline media. It was shown that all metal ad-atoms enhanced the electrocatalytic oxidation of ethylene glycol. An increase in the current density, which was close to diffusion-limited current densities with the best foreign metals (Pb and Bi), could be explained by the bi-functional theory of electrocatalysis. Smirnova et al. [38] examined the potential shifts of a Pt electrode and one modified with ad-atoms under the open-circuit condition. It was shown that the improvement in the electrocatalytic oxidation of ethylene glycol on the tin-modified Pt electrode in alkaline media was l - l.5 orders of magnitude; while, the lead-modified Pt electrode accelerated the oxidation reaction by two orders of magnitude.

3.1.2. Palladium

The monometallic and bimetallic Pd-based nanomaterials have emerged as electrocatalysts for the oxidation of various alcohols in alkaline media. Hence, Pd or Pd-based electrodes for the electrocatalytic oxidation of ethylene glycol in alkaline media have been extensively investigated [24, 39-45]. Xie et al. [24] compared the electrocatalytic oxidation of various alcohols on Pt and Pd electrodes via a three-electrode cell, including methanol, ethanol, n-propanol, isopropanol, ethylene glycol and glycerol, and found that the electro-oxidation of various alcohols on the Pd electrode followed the sequence of n-propanol > isopropanol > ethanol > ethylene glycol > glycerol > methanol. Dalbay et al. [39] investigated the electrocatalytic oxidation of ethylene glycol on Pt-Pd alloyed electrodes with different compositions in alkaline media via cyclic voltammetry. They found that as compared to pure metals, the electrocatalytic activity was enhanced resulting from a synergistic effect in electrocatalysis. Wang et al. [40] investigated the adsorption and oxidation pathways of ethylene glycol on polycrystalline Pd surfaces in alkaline media via in-situ FTIR spectroscopy and cyclic voltammetry. It was shown that Pd exhibited a high electrocatalytic activity toward the ethylene glycol oxidation in alkaline media with low onset potentials and high current densities, which would be affected by the pH and the supporting electrolyte. It was also shown that the pathways of the electrocatalytic oxidation of ethylene glycol were affected by the pH, as shown in Table 1. In addition, Pd showed high activity toward the ethylene glycol oxidation in strong alkaline solutions and then a mechanism was proposed for the electrocatalytic oxidation of ethylene glycol on the Pd surface, as illustrated in Fig. 1b. As a result of the fact that Pd is not prone to breaking the C-C bond in ethylene glycol, the use of Pd for the ethylene glycol oxidation increases the oxalate production, alleviates electrode poisoning by CO species, and thus enhances the electrocatalytic stability. For this reason, it is feasible to use Pd as the anode electrocataslyts in fuel cells that can simultaneously generate electricity and produce chemicals in a sustainable way

[41-43]. Bambagioni et al. [44] investigated the oxidation of ethylene glycol on a Pd electrode in alkaline media via in-situ FTIR spectroscopy. It was shown that the electrocatalytic oxidation of ethylene glycol on the Pd electrode was dramatically affected by the pH. Specifically, at pH below 12, carbonate was detected; while, glycolate, carbonate and oxalate were produced almost simultaneously at a potential of about 0.4 V (vs. RHE) at higher pH. In addition, at potentials higher than 0.9 V, glycolate could be further oxidized to oxalate and carbonate. Lin et al. [45] investigated the electrocatalytic oxidation of ethylene glycol on the polycrystalline Pd electrode in alkaline media via in-situ FTIR reflection spectroscopy and examined the effect of ethylene glycol concentration on the reaction pathways. They determined that the reaction order of ethylene glycol oxidation was near 0.5. It was shown from the in-situ FTIR results that the reaction pathways and the product distributions were strongly dependent of the ethylene glycol concentration. They found that the main products gradually varied from carbonate, oxalate, glyoxylate, to glycolate with the ethylene glycol concentration. In addition, the competitive adsorption between ethylene glycol/intermediates and water inhibited the formation of oxygen species from water dissociation, which was regarded to be a key oxygen donor for the deep oxidation of ethylene glycol.

3.1.3. Gold

It is known that Au is also a good candidate for the electrocatalytic oxidation of various alcohols in alkaline media. Hence, Au or Au-based electrodes for the electrocatalytic oxidation of ethylene glycol in alkaline media have been extensively studied [28, 31, 46-48]. Beden et al. [46] investigated the oxidation of several organic compounds on Au in both acid and alkaline media via cyclic voltammetry. It was shown that in alkaline media, Au was an excellent electrocatalyst, particularly for the oxidation of the aldehyde functional group and the alcohol group. Ureta-Zanartu et al. [47] studied that the electrocatalytic oxidation of methanol and ethylene glycol on Au and poly NiTSPc/Au/Q electrodes in the carbonate/hydrogen carbonate buffer electrolyte (pH=11) via cyclic voltammetry and an electrochemical quartz crystal microbalance (EQCM). They found that ethylene glycol was oxidized on Au at a high rate because it was adsorbed rather strongly on the Au surface. Adzic et al. [48] investigated the electrocatalytic oxidation of ethylene glycol on single crystal gold electrodes in alkaline media. They found that (1) ethylene glycol was not oxidized on the $AuOH^-$, or oxide-free, metallic gold surface; (2) a pronounced structural sensitivity of the oxidation of ethylene glycol on Au was observed; and (3) the participation of the AuOH species in the electrocatalytic oxidation of ethylene glycol confirmed one step in the mechanism of the oxidation of ethylene glycol on Au. Chang et al. [28] investigated the oxidation of ethylene glycol on the Au surface in alkaline media via real-time FTIR spectroscopy and cyclic voltammetry. They found that like the reactions on Pt and Pd, the partially oxidized C_2 intermediates were formed in the electrocatalytic oxidation of ethylene glycol on Au, followed by a further oxidation to oxalate and carbonate. Carbonate was produced predominantly from the further oxidation of the glyoxal. Angelucci et al. [31] investigated the effect of cations on the electrocatalytic oxidation of glycerol and ethylene glycol on Pt and Au in alkaline media via cyclic voltammetry and chronoamperometry. It was shown that radically different from the behaviors on Pt, the effect of OH_{ad}-$M^{+}(H2O)_{x}$ clusters on the electrocatalytic oxidation on Au was not significant.

3.1.4. Others

In addition to noble metals (Pt, Pd and Au), non-precious metals, such as nickel (Ni) and cobalt (Co), have emerged as electrocatalysts for the electrocatalytic oxidation of small organic molecules in alkaline media [28, 49]. Chang et al. [28] investigated the oxidation of ethylene glycol on the Ni surface via real-time FTIR spectroscopy and cyclic voltammetry. It was shown that the electrocatalytic oxidation of ethylene glycol on Ni exhibited a selective production of formate followed by a further oxidation to carbonate, suggesting that the C-C bond cleavage occurred readily on the Ni surface. Pletcher et al. [49] investigated the mechanism of the oxidation of organic species (ethylene glycol, glycerol, etc.) on a Co electrode and found that the mechanism was similar to that on a Ni electrode.

3.2. Electrocatalysts

3.2.1. Pt and Pt-based electrocatalysts

Pt/Pt-based materials have been widely used as electrocatalysts for the electrocatalytic oxidation of ethylene glycol in acid media [13]. For this reason, numerous efforts have been devoted to the development of Pt/Pt-based electrocatalysts for the ethylene glycol oxidation in alkaline media [50-53]. Xin et al. [50] prepared Pt/C via a modified solution-phase reduction method and investigated the electrocatalytic oxidation of ethylene glycol in alkaline media via a three-electrode cell. It was shown that glycolic acid, oxalic acid, and formic acid were sequentially produced from ethylene glycol oxidation on Pt/C. The presence of oxalic acid was attributed to the fact that oxalic acid was stable on Pt/C and difficult to be further oxidized to carbon dioxide. Formic acid was produced preferably from the direct C-C bond cleavage of ethylene glycol on Pt/C. In addition, the results also were examined by a single alkaline DEGFC using Pt/C electrocatalysts on the anode. It was found that oxalic acid and formic acid were detected when ethylene glycol was used as fuel; while, there was no formic acid detected when glycolic acid was fed as fuel. It has been demonstrated that the co-presence of metals/metal oxides can remarkably affect electrocatalytic activity and stability [13]. Kim et al. [51] prepared Pt-Ag nanotubes via the partial galvanic exchange of Pt on Ag nanowires and investigated the electrocatalytic oxidation of ethylene glycol and glycerol in alkaline media. It was demonstrated that the electrocatalytic activity was substantially enhanced as compared with Pt nanotubes, commercial Pt black or Pt/C electrocatalysts, in terms of peak current densities, onset potentials and anti-poisoning properties. The improvement was attributed to the tailored geometric and electronic structures of the Pt-Ag nanotubes. Xu et al. [52, 53] investigated the electrocatalytic oxidation of methanol, ethanol, glycerol and ethylene glycol on Pt-CeO_2/C electrocatalysts in alkaline media. The electrode with the weight ratio (Pt to CeO_2) of 1.3:1 (Pt loading: 0.30 mg cm^{-2}) exhibited the highest electrocatalytic activity for the oxidation of ethanol, glycerol and ethylene glycol. They found that the Pt-CeO_2/C electrocatalysts could significantly improve the performance, in terms of the electrocatalytic activity and the anti-poisoning property, both of which were rendered by the synergistic effect.

3.2.2. Pd and Pd-based electrocatalysts

It has been demonstrated that Pd/Pd-based electrocatalysts are more active than Pt/Pt-based electrocatalysts for the oxidation of small organic molecules in alkaline media [14]. Hence, many efforts have been devoted to developing Pd and Pd-based electrocatalysts for the ethylene glycol oxidation in alkaline media and significant progress has been made [44, 54-65]. Pattabiraman et al. [54] prepared Pd/C electrocatalysts via the reduction method using various reducing agents. They evaluated the electrocatalytic activity for the oxidation of hydrogen, methanol, formaldehyde and ethylene glycol, and the reduction of oxygen in alkaline media. It was shown that Pd/C electrocatalysts exhibited high electrocatalytic activity for the oxidation of hydrogen and ethylene glycol. Li et al. [55] developed a simple method to prepare the Pd nanodendrites anchored on the reduced graphene oxide (Pd/rGO) at room temperature. It was shown that the prepared electrocatalysts improved the CO tolerance, enhanced the electrocatalytic activity, and exhibited better stability for ethylene glycol and glycerol oxidation in alkaline media as compared to commercial Pd black and Pd/C electrocatalysts. In addition, Cherevko et al. [56] prepared Pd foam with the roughness factor of more than 1000 and a specific surface area of 60 m^2 g^{-1} via electrodeposition, which consisted of dendrites and branches. They found that the Pd foams showed high electrocatalytic activity toward the oxidation of ethanol and ethylene glycol. It has been demonstrated that the support in electrocatalysts can significantly affect the performance [19]. Xu et al. [57] prepared carbon microspheres (CMS) supported Pt and Pd electrocatalysts for electrocatalytic oxidation of alcohols (methanol, ethanol and ethylene glycol) in alkaline media. It was shown that Pt/CMS and Pd/CMS electrocatalysts resulted in better performance for all alcohols than carbon supported electrocatalysts did. In addition, the activity order of electrocatalytic oxidation of alcohols on Pt/C and Pt/CMS was ethylene glycol > methanol > ethanol; while, the activity order on Pd/C and Pd/CMS was ethanol > ethylene glycol > methanol.

In addition, attempts have also been made to combine Pd with other metals to improve the electrocatalytic activity for the ethylene glycol oxidation in alkaline media [14]. Ramulifho et al. [58] prepared Pd-M bimetallic electrocatalysts (M: Ni or Sn) supported on sulfonated multi-walled carbon nanotubes (SF-MWCNT) for the electrocatalytic oxidation of ethylene glycol in alkaline media. The bimetallic electrocatalysts (Pd-Sn/SF-MWCNT or Pd-Ni/SF-MWCNT) showed better electrocatalytic activity toward the ethylene glycol oxidation than the Pd/SF-MWCNT did. In addition, the ethylene glycol oxidation on Pd-Ni/SF-MWCNT was more stable than that on Pd-Sn/SF-MWCNT. Serov et al. [59] prepared unsupported Pd-In electrocatalysts via the sacrificial support method. They found that the electro-oxidation of ethylene glycol and glycerol on Pd-In_3 electrocatalysts was significantly higher than those reported in the literature. Kannan et al. [60] prepared Pd-Ni bimetallic nanoparticles coated onto manganite (MN) electrocatalysts for the electrocatalytic oxidation of ethylene glycol and glycerol in alkaline media, where MN nanorods were prepared via the hydrothermal method and Pd-Ni was coated on the rods via an in-situ reduction method. It was shown that the prepared electrocatalysts in the electrolyte solution containing 9 M KOH and 6 M ethylene glycol exhibited the highest electrocatalytic activity. Bambagioni et al. [44] studied the electrocatalytic oxidation of ethylene glycol on nanostructured Pd-based electrocatalysts in alkaline media via cyclic voltammetry. The experimental results implied that the nanostructured electrocatalysts, including Pd-(Ni-Zn)/C, Pd-(Ni-Zn-P)/C, and Pd/C, were much more active than the smooth Pd electrode and correspondingly resulted in different product distributions. It was shown that Pd/C was the most selective electrocatalyst producing glycolate; while, glycolate, oxalate and carbonate were obtained with Pd-(Ni-Zn)/C or Pd-(Ni-Zn-P)/C. In addition, carbonate was predominately produced from the oxidation of glycolate; while, oxalate was mainly produced from the direct oxidation of ethylene glycol. After that, Marchionni et al. [61] studied the electrocatalytic oxidation of ethylene glycol and glycerol in alkaline media via passive and active fuel cells using Pd-(Ni-Zn)/C as the anode electrocatalyst. The results showed that Pd-(Ni-Zn)/C exhibited excellent electrocatalytic activity in terms of the peak current density. In addition, MEAs were fabricated by using Pd-(Ni-Zn)/C as the anode electrocatalysts (Pd loading: 1.0 mg cm^{-2}), Fe-Co/C as the cathode electrocatalysts, and an AEM (Tokuyama A201). As shown in Fig. 2, the constructed fuel cell exhibited an open-circuit voltage (OCV) of 0.9 V and a peak power density of 95 mW cm^{-2} at 80^{o}C. Fashedemi et al. [62]

investigated the electrocatalytic oxidation of alcohols (ethanol, ethylene glycol and glycerol) on palladium-based core-shell electrocatalysts (FeCo@Fe@Pd/C) synthesized via the microwave-induced top-down nanostructuring and decoration synthetic strategy. The FeCo@Fe@Pd/C exhibited a remarkable performance for three alcohols, among which the activity of the ethylene glycol oxidation was found to be the best, resulting from the low resistance of charge transport. Fashedemi et al. [63] investigated the oxidation of ethylene glycol and glycerol on FeCo@Fe@Pd/MWCNT-COOH and FeCo@Fe@Pd/MWCNT-SO_3H in alkaline media. It was proved that the surface functional groups (mainly -COOH and -SO_3H) on MWCNTs played a critical role in the physicochemical properties of the FeCo@Fe@Pd electrocatalysts. As compared to FeCo@Fe@Pd/MWCNT-SO_3H, the FeCo@Fe@Pd/MWCN-COOH showed smaller nanoparticles, more uniform dispersion on the support, larger electrochemical surface area and thus enhanced the electrocatalytic activity toward the oxidation reactions.

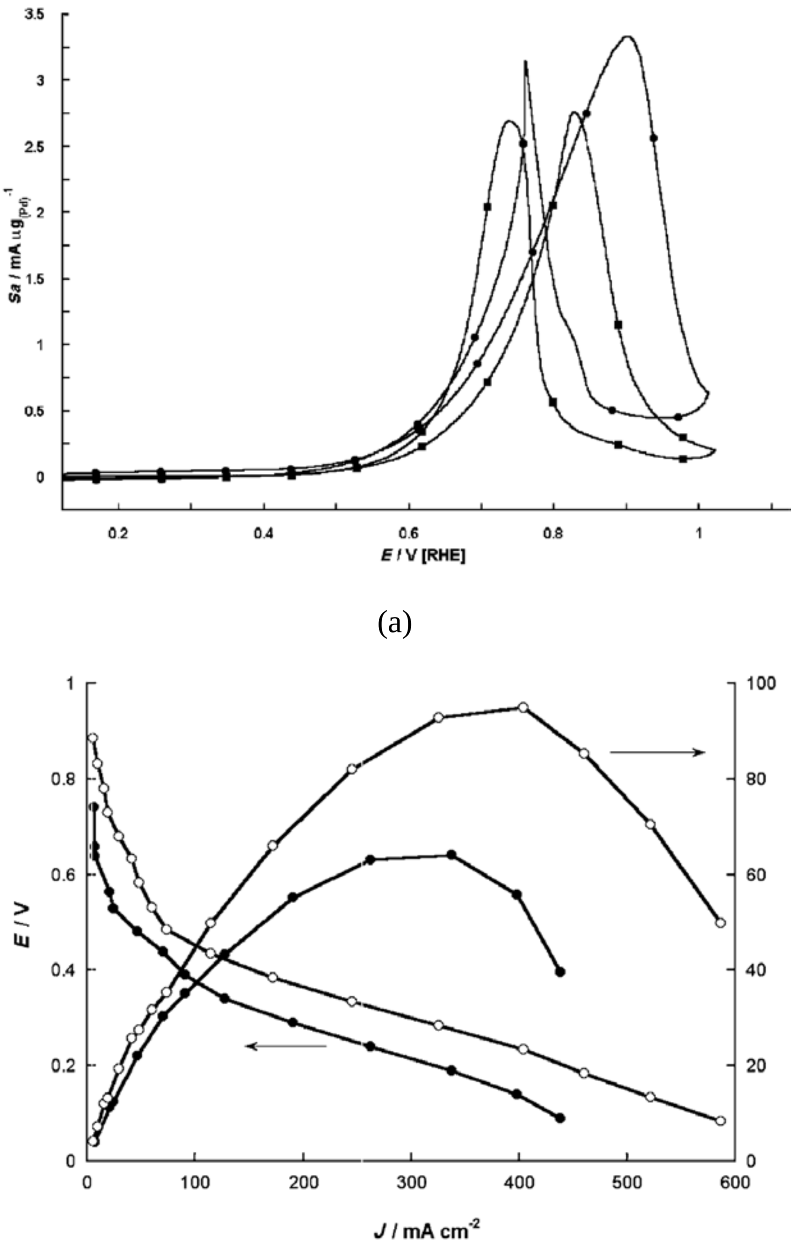

(a)

(b)

Fig. 2 (a) Cyclic voltammograms of ethylene glycol electro-oxidation on Pd-(Ni-Zn)/C (•) and Pd/C (■) electrodes and (b) polarization and power density curves for direct ethylene glycol fuel cells using Pd-(Ni-Zn)/C (o) and Pd/C (•) as anode electrocatalysts at 80°C [61]. Reproduced with permission from Wiley.

It has been demonstrated that co-presence of metal oxides can remarkably affect electrocatalytic activity and stability [13]. Shen et al. [64] prepared Pd/C with nanocrystalline oxides (CeO_2, Co_3O_4, Mn_3O_4 and NiO) electrocatalysts via the intermittent microwave heating, and studied the electrocatalytic oxidation of methanol, ethanol, glycerol and ethylene glycol on various metal oxides promoted Pd/C electrocatalysts in alkaline media. It was shown that those electrocatalysts were superior to Pt-based electrocatalysts in terms of the electrocatalytic activity and poison tolerance. Xu et al. [65] investigated Pt/C, Pd/C and metal oxide-promoted Pd/C electrocatalysts (oxide: CeO_2, NiO, Co_3O_4 and Mn_3O_4) for electrocatalytic oxidation of methanol, ethanol, ethylene glycol and glycerol in alkaline media. Among those electrocatalysts, Pd/C exhibited low activity and poor stability for the alcohol oxidation. The addition of metal oxides (CeO_2, NiO, Co_3O_4 and Mn_3O_4), however, significantly enhanced the electrocatalytic activity and stability. Among the modified catalysts, Pd-Co_3O_4/C showed the highest activity for the electrocatalytic oxidation of methanol, ethylene glycol and glycerol.

3.2.3. Au and Au-based electrocatalysts

Au/Au-based electrocatalysts for the electrocatalytic oxidation of ethylene glycol in alkaline media have been extensively investigated [66-69]. Yongprapat et al. [66] prepared the metal oxide-promoted Au-based electrocatalysts (oxide: CeO_2, Fe_2O_3

and RuO_2) for the electrocatalytic oxidation of ethylene glycol via polyvinyl alcohol (PVA) protection method and their activity and stability were investigated via cyclic voltammetry and chronoamperometry, respectively. They found that both Fe_2O_3- and RuO_2-promoted electrocatalysts resulted in higher current densities than the Au/C electrocatalysts did. Xin et al. [67] prepared Au/C nanoparticles via a modified solution-phase reduction method, and investigated their electrocatalytic activity of the ethylene glycol oxidation in alkaline media via a three-electrode cell. It was shown that glycolic acid and formic acid were detected, in which glycolic acid was the primary product and there was no oxalic acid production. Like Pt/C, formic acid was produced from the direct C-C bond cleavage in ethylene glycol on Au/C electrocatalysts. In addition, the results were also examined by a single alkaline DEGFC using Au/C as the anode electrocatalysts and they found the major product of the electrocatalytic oxidation of ethylene glycol was glycolic acid (> 98%). Jin et al. [68] prepared Pt-Au nanoparticles via chemical reduction and investigated their electrocatalytic activities of the ethylene glycol oxidation in alkaline, neutral, and acid media via cyclic voltammetry. It was found that the Pt-Au electrocatalysts exhibited high electrocatalytic activity and stability in alkaline media, originating from the presence of oxidation peaks at low potentials with high current densities. In addition, it was found that a higher alkali concentration was favorable for the ethylene glycol oxidation. They concluded that the high electrocatalytic activity of Pt-Au electrocatalysts was attributed to the synergistic effect on electrocatalysis and an increase in the active surface area. Brandalise et al. [69] prepared a series of electrocatalsyts for the electrocatalytic oxidation of ethylene glycol, including Pd/C, Au/C, Au-Bi/C, Pd-Au/C and Pd-Au-Bi/C, via borohydride reduction method. They showed that the Pd-Au-Bi/C electrocatalyst resulted in the highest electrocatalytic activity.

3.2.4. Others

Currently, only a few non-precious metals have been regarded as electrocatalysts for the electrocatalytic oxidation of ethylene glycol in alkaline media [28, 49, 70]. Ewe et al. [70] evaluated ethylene glycol as fuel for alkaline fuel cells by using Raney nickel as electrocatalysts. They confirmed that ethylene glycol could be oxidized at high current densities at elevated temperatures. The intermediate, glycolate, could be further oxidized by Raney nickel electrocatalysts to produce oxalate at temperatures above 60 °C. In addition, about six electrons per ethylene glycol molecule were found to be released in the ethylene glycol oxidation. The Raney electocatalysts showed good durability and did not exhibit the poisoning effect.

In summary, Sections 3.1 and 3.2 have summarized and discussed the past investigations on the electrocatalytic oxidation and electrocatalysts of ethylene glycol mainly on three types of electrode/electrocatalyst, i.e., Pt/Pt-based, Pd/Pd-based and Au/Au-based, suggesting that the electrocatalytic activity, stability and durability of electrocatalysts need to be further enhanced. In addition, non-precious metals/metal oxides, such as Ni and Co, should also be considered as a promising candidate for electrocatalysts toward the ethylene glycol oxidation in alkaline media.

4. Single-cell performance

For the given materials, the fuel cell performance only depends on the cell design parameters and the operating parameters [71]. As summarized in Table 2, it can be seen that the power density has been substantially boosted from 1.3 mW cm^{-2} to 112 mW cm^{-2} in recent years. Matsuoka et al. [72] fabricated and tested alkaline DOFCs running on various polyhydric alcohols, which used Pt-Ru/C as anode electrocatalysts with a loading of 4.0 mg cm^{-2}, an AEM with a thickness of 240 μm, and Pt/C as cathode electrocatalysts with a loading of 1.0 mg cm^{-2}, respectively, as illustrated in Fig. 3a. The peak power densities of fuel cells running on various polyhydric alcohols (the fuel solution containing 1.0 M fuel + 1.0 M KOH) were in the following order: ethylene glycol > glycerol > methanol > erythritol > xylitol, where the alkaline DEGFC resulted in an OCV of about 0.8 V and a peak power density of 9.5 mW cm^{-2} at 50^{o}C (see Figs. 3b and 3c). Also, they fabricated an alkaline DEGFC using the Ag/C as cathode electrocatalysts and it was tested with an ethylene glycol concentration ranging from 1.0 M to 5.0 M and at 50^{o}C. Although the OCV of the fuel cell with the Ag/C electrocatalysts reached 0.65 V, which was about 0.15 V lower than the fuel cell with the Pt/C electrocatalysts, the fuel cell performance using Ag/C could be improved by increasing the ethylene glycol concentration. It was shown that the fuel cell performance achieved by 3.0- or 5.0-M operation was comparable to that using Pt/C electrocatalysts at current densities higher than 40 mA cm^{-2}. It was demonstrated that the peak power densities were 8.1 mW cm^{-2} and 7.4 mW cm^{-2} with 3.0 M and 5.0 M ethylene glycol, respectively. More importantly, it was indicated that the use of Ag/C electrocatalysts on the cathode of alkaline DOFCs not only resulted in a good fuel cell performance, but also allowed the high-concentration fuel to be fed, which is particularly promising for portable applications.

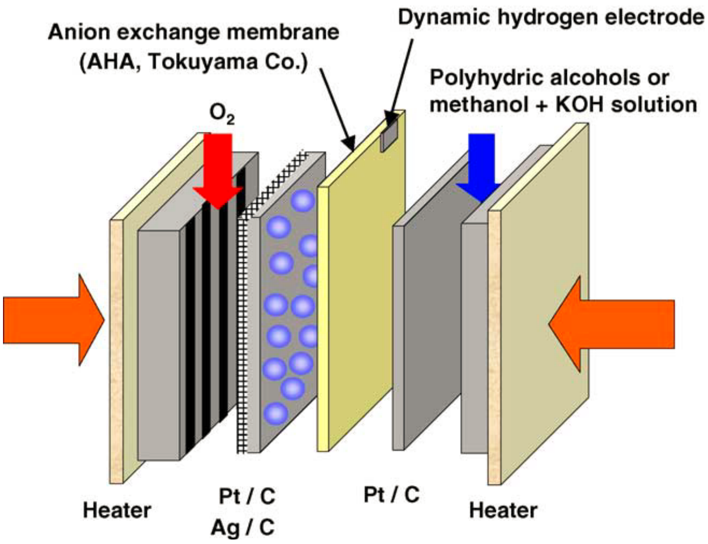
Anion exchange membrane
(AHA, Tokuyama Co.)
Dynamic hydrogen electrode
Polyhydric alcohols or
methanol + KOH solution
O2
Heater
Pt / C
Ag / C
Pt / C
Heater

(a)

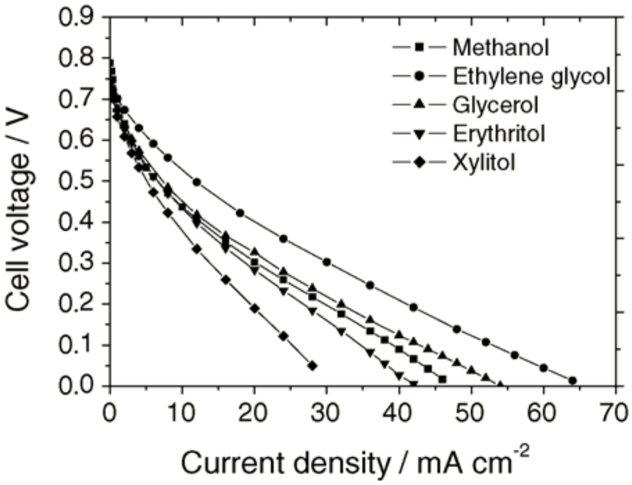
Cell voltage / V
Current density / mA cm-2
0.0
0.1
0.2
0.3
0.4
0.5
0.6
0.7
0.8
0.9
0
10
20
30
40
50
60
70
Methanol
Ethylene glycol
Glycerol
Erythritol
Xylitol

(b)

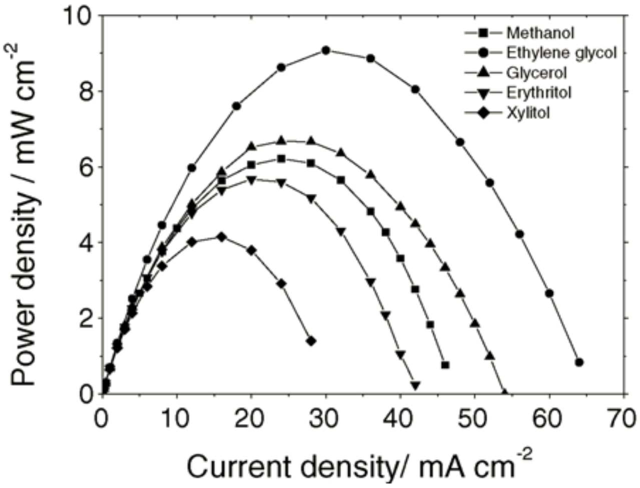
Power density / mW cm-2
Current density/ mA cm-2
0
2
4
6
8
10
0
10
20
30
40
50
60
70
Methanol
Ethylene glycol
Glycerol
Erythritol
Xylitol

(c)

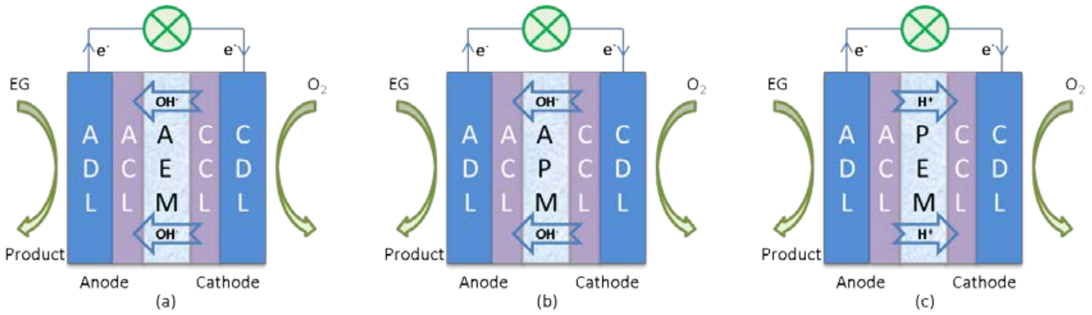
e-
e-
EG
O2
Product
A D L
A C L
A E M
C C L
C D L
OH-
OH-
Anode
Cathode
(a)
A P M
(b)
P E M
H+
H+
(c)

(d)

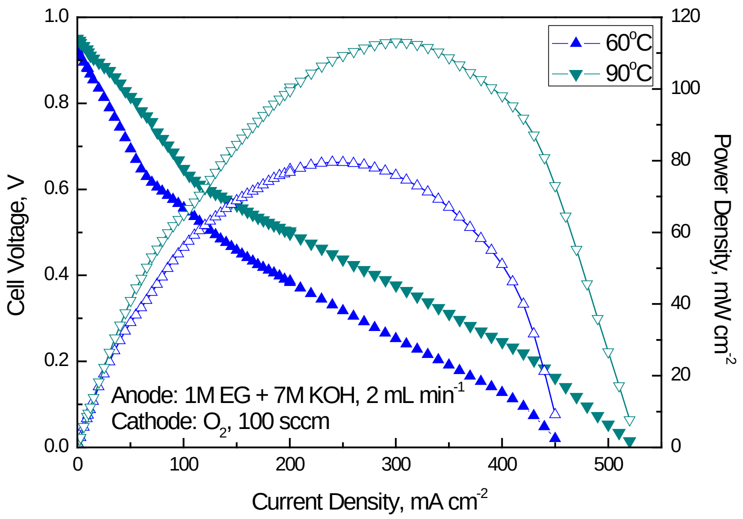
60°C
90°C
Anode: 1M EG + 7M KOH, 2 mL min-1
Cathode: O2, 100 sccm
Cell Voltage, V
Power Density, mW cm-2
Current Density, mA cm-2
1.0
0.8
0.6
0.4
0.2
0.0
0
100
200
300
400
500
120
100
80
60
40
20
0

(e)

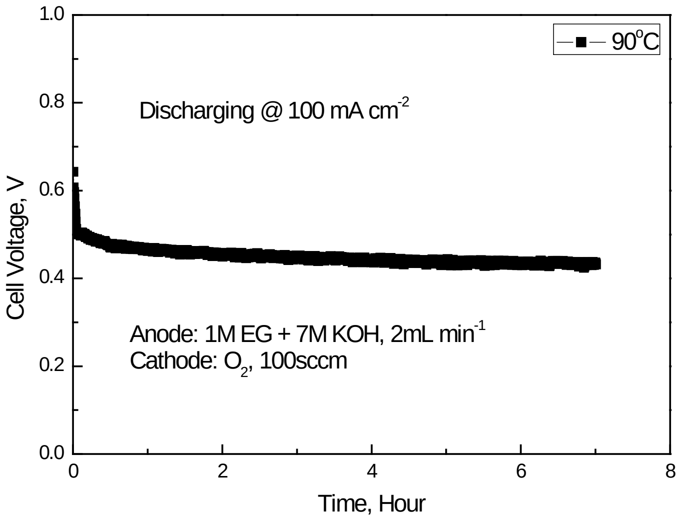
90°C
Discharging @ 100 mA cm-2
Anode: 1M EG + 7M KOH, 2mL min-1
Cathode: O2, 100sccm
Cell Voltage, V
Time, Hour
1.0
0.8
0.6
0.4
0.2
0.0
0
2
4
6
8

(f)

Fig. 3 (a) Schematic of a direct alkaline fuel cell using an anion exchange membrane; (b) polarization and (c) power density curves of alkaline direct alcohol fuel cells using polyhydric alcohols at 50^{o}C [72]; (d) schematic of various types of direct ethylene glycol fuel cell; (e) polarization and power density curves at 60^{o}C and 90^{o}C; and (f) constant-current discharging behavior at 90^{o}C [74]. Reproduced with permission from Elsevier.

Demarconnay et al. [35] investigated the electrocatalytic oxidation of ethylene glycol on the Pt-based electrocatalysts in alkaline media. It was found that the addition of Bi to Pt decreased the onset potential of the ethylene glycol oxidation by about 70 mV and resulted in higher current densities. They explained that the enhancement of the electrocatalytic activity in the presence of Bi was attributed to the bi-functional theory in electrocatalysis; while, the addition of Pd reduced the poisoning effect [36]. They further prepared the ternary Pt-Pd-Bi/C electrocatalysts and found that they did not change the onset potentials, but increased the current densities as compared to the binary Pt-Bi electrocatalysts. The three types of electrocatalyst (with a loading of 2.0 mg cm^{-2}), Pt/C, Pt-Bi/C and Pt-Pd-Bi/C, were respectively used to form three anodes for alkaline DEGFCs. By using an AEM (ADP-Morgane$^{®}$) with a thickness of 150-160 μm and Pt/C as the cathode electrocatalysts with a loading of 2.0 mg cm^{-2}, it turned out that the OCV were 0.66 V (Pt/C), 0.83 V (Pt-Bi/C), and 0.81 V (Pt-Pd-Bi/C) and the peak power densities were 19 mW cm^{-2} (Pt/C), 22 mW cm^{-2} (Pt-Bi/C), and 28 mW cm^{-2} (Pt-Pd-Bi/C) at 20°C. Recently, An et al. [73] designed, fabricated, and tested an alkaline DEGFC, which used Pd-Ni/C electrocatalysts on the anode (1.0 mg cm^{-2}), an AEM (Tokuyama A201) with a thickness of 28 μm, and non-platinum HYPERMEC^{TM} electrocatalysts (Acta) on the cathode (1.0 mg cm^{-2}). They further investigated the effects of the operating parameters on the fuel cell performance, including the reactant concentrations, reactant supply flow rates at the anode and cathode, and the operating temperature. It was found that the operating parameters, including the reactant concentrations and the operating temperature, have significant influence on the cell performance. After optimization, it turned out that a peak power density of 67 mW cm^{-2} at 60°C was achieved when the fuel cell was operated with an aqueous solution containing 1.0 M ethylene glycol and 7.0 M KOH fed to the anode at a flow rate of 2.0 mL min^{-1} and the dry pure oxygen fed to the cathode at a flow rate of 100 standard cubic centimeter per minute (sccm). They concluded that the improvement in the fuel cell performance was mainly attributed to the enhanced kinetics of both the ethylene glycol oxidation reaction and ORR rendered by alkaline media. Xin et al. [67] fabricated an alkaline DEGFC with Pt/C or Au/C as anode electrocatalysts (1.0 mg cm^{-2}), an AEM with a thickness of 28 μm (Tokuyama A201), Fe-Cu-N_4/C (Acta 4020) as cathode electrocatalysts (1.0 mg cm^{-2}). The fuel cell with

Pt/C electrocatalysts resulted in a peak power density of 71.0 mW cm^{-2} at 50^{o}C, which was much higher than that with the Au/C (7.3 mW cm^{-2}) did. More recently, An et al. [74] developed an alkaline DEGFC with an alkali-doped polybenzimidazole membrane with a thickness of 30 μm as the AEM, by which the operation of this fuel cell system at temperatures higher than 60^{o}C was allowed, as shown in Fig. 3d. The fuel cell fabricated with Pd-Ni/C electrocatalysts at the anode (1.0 mg cm^{-2}) and non-platinum HYPERMEC^{TM} electrocatalysts (Acta) at the cathode (1.0 mg cm^{-2}). It was found that a peak power density of 112 mW cm^{-2} was achieved at a current density of 300 mA cm^{-2} when operated at 90^{o}C with an aqueous solution of 1.0 M ethylene glycol + 7.0 M KOH at a flow rate of 2.0 mL min^{-1} and dry pure oxygen at a flow rate of 100 sccm, as shown in Fig. 3e. The change of the oxidant from pure oxygen to the air decreased the peak power density to 92 mW cm^{-2}. It was suggested that the performance improvement is attributed not only to the superior electrochemical kinetics of both ethylene glycol oxidation and oxygen reduction reactions in alkaline media, but also the increased operating temperature rendered by the use of an alkali-doped polybenzimidazole membrane. In addition, they also investigated the discharging behavior at a constant current density of 100 mA cm^{-2} and found that there was no fluctuation in the cell voltage during the 7-h continuous operation at 90^{o}C, as shown in Fig. 3f. It should be mentioned that the fuel cells that purely relied on an AEM and corresponding ionomers to conduct hydroxide ions were also investigated [75-77]. Varcoe et al. [77] fabricated direct alcohol fuel cells by using two newly developed AEMs, unsupported Pt-Ru as anode electrocatalysts with a loading of 4.0 mg cm^{-2}, and unsupported Pt black as cathode electrocatalysts with a loading of 4.0 mg cm^{-2}, respectively. It was found that the peak power densities of fuel cells running on ethylene glycol were 1.99 mW cm^{-2} and 1.57 mW cm^{-2} when assembled with two membranes, respectively.

In summary, the performance of alkaline DEGFCs with various electrocatalytic and membrane materials, as well as operating parameters has been summarized and discussed. It is clear that without an additional liquid electrolyte, the fuel cell cannot result in a satisfactory performance, primarily because of the low conductivity of state-of-the-art AEMs and corresponding ionomers. The previous investigations indicate that an effective approach to improve the fuel cell performance is to add liquid electrolyte (typically KOH) in the fuel solution. However, the presence of the liquid electrolyte also brings several issues: i) carbonate production via the reaction between the crossovered alkali and carbon dioxide from the air will reduce the ionic conductivities of AEMs and corresponding ionomers; ii) the carbonate precipitation will reduce the hydrophobicity of the porous electrode, thus breaking the balance of mass transport between water and oxygen; and iii) the poor chemical stability of

AEMs in strong alkaline environment. It is seen that all above-mentioned issues are caused by the added alkali so that the solution to those problems is to operate a fuel cell that purely relies on the solid-state electrolyte and corresponding ionomers to conduct hydroxide ions, so-called alkali-free or liquid-electrolyte-free alkaline fuel cells. For this reason, the future direction should be to develop the high-conductivity AEM materials.

5. Innovative system designs

In addition, there are some other types of fuel cell running on ethylene glycol, including solid oxide fuel cells (SOFC), redox fuel cells, micro/nanofluidic fuel cells, as well as an energy-storage system using ethylene glycol as energy carrier.

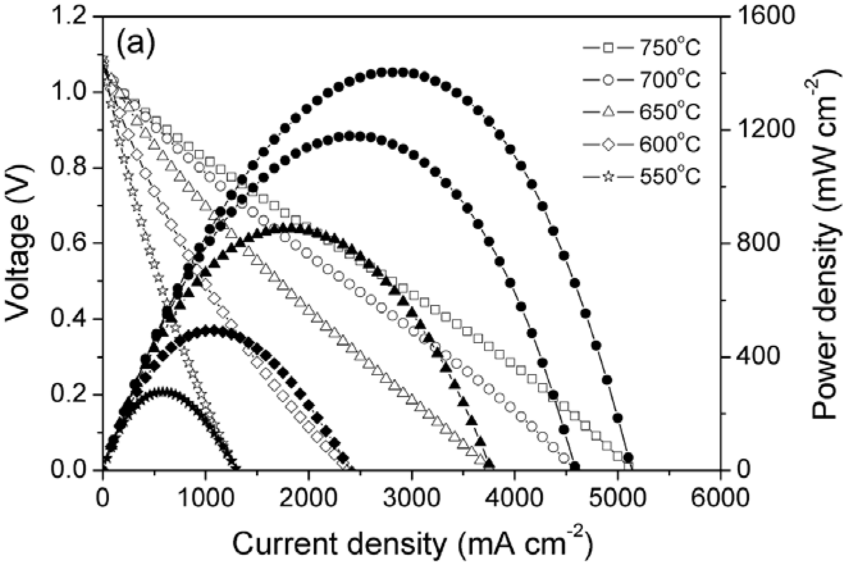
(a)
Voltage (V)
Power density (mW cm^{-2})
Current density (mA cm^{-2})
750°C
700°C
650°C
600°C
550°C
0.0
0.2
0.4
0.6
0.8
1.0
1.2
0
400
800
1200
1600
0
1000
2000
3000
4000
5000
6000

(a)

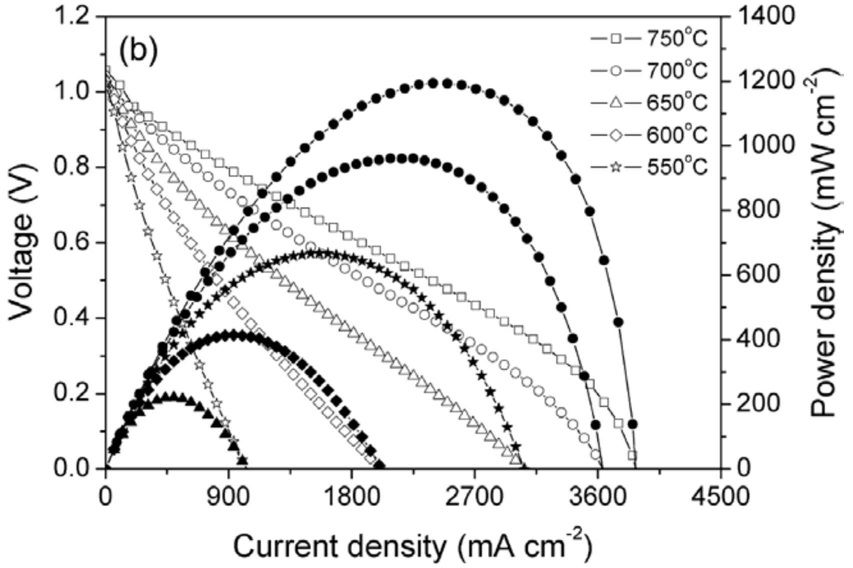
(b)
Voltage (V)
Power density (mW cm^{-2})
Current density (mA cm^{-2})
750°C
700°C
650°C
600°C
550°C
0.0
0.2
0.4
0.6
0.8
1.0
1.2
0
200
400
600
800
1000
1200
1400
0
900
1800
2700
3600
4500

(b)

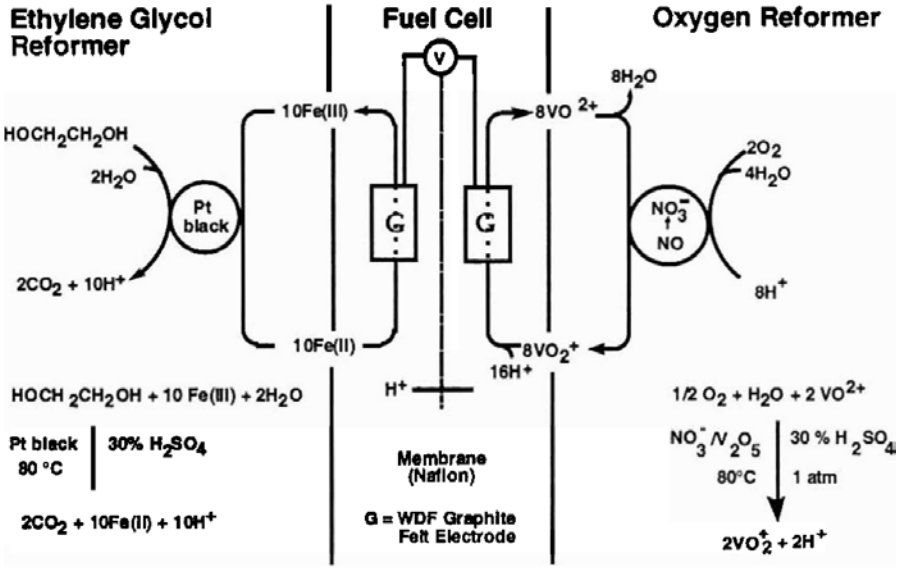

(c)

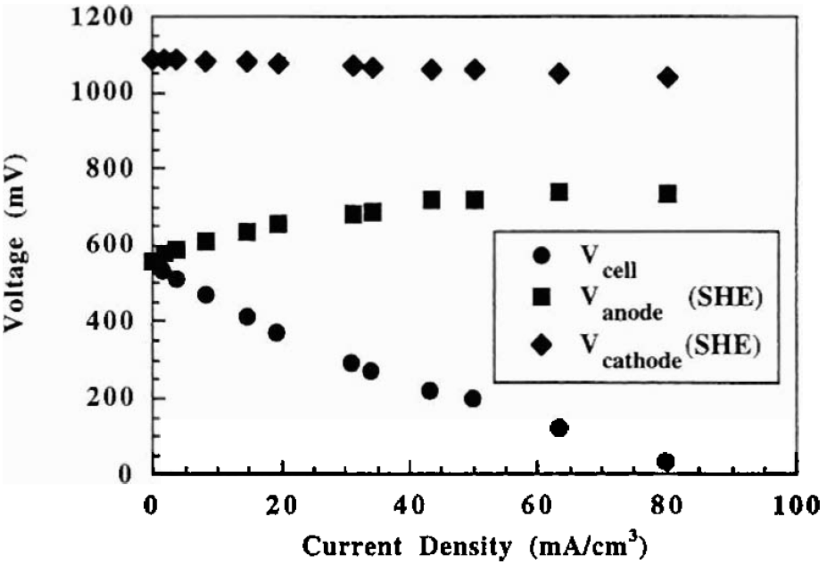

(d)

Fig. 4 Polarization and power density curves of solid oxide fuel cells at different temperatures running on: (a) hydrogen and (b) ethylene glycol steam [78]; (c) schematic of a redox fuel cell running on ethylene glycol and (d) polarization curvres and electrode potentials [79]. Reproduced with permission from Elsevier.

5.1. Solid oxide fuel cells running on ethylene glycol

In addition to feeding ethylene glycol to low-temperature fuel cells, Qu et al. [78] recently demonstrated that ethylene glycol could be used as a fuel in solid oxide fuel cells with conventional nickel yttria-stabilized zirconia (Ni-YSZ) cermet anodes for power generation. Among various fuels, including ethylene glycol, glycerol, ethanol and methane, the SOFC running on ethylene glycol was found to be the best in terms of carbon deposition. It was also found that the fuel cell operated with ethylene glycol steam as fuel could result in a peak power density of 1200 mW cm^{-2} at 750^{o}C, as shown in Figs. 4a and 4b, which was comparable with that achieved by a SOFC running on hydrogen. In addition, it was found that there was no significant decay in the cell voltage when operated at 750^{o}C with a current density of 400 mA cm^{-2} for 200 h. Therefore, it is suggested that it is feasible to use ethylene glycol as fuel in SOFCs for future power generation.

5.2. Redox fuel cells running on ethylene glycol

Gorman et al. [79] proposed a redox fuel cell with the respective redox couple at the anode and cathode regenerated by the fuel (ethylene glycol) and the oxidant (oxygen), as illustrated in Fig. 4c. Both the anode and cathode, separated by a Nafion membrane, were consisted of graphite felt that was pre-treated by the boiling concentrated nitric acid for 15 min. Two redox couples, Fe(II)/Fe(III) and V(IV)/V(V), were used at the anode and the cathode, respectively. On the anode, the redox ions

(Fe^{2+}) are oxidized by releasing electrons according to [80]:

$$Fe^{2+} \rightarrow Fe^{3+} + e^{-} \qquad E_a^0 = 0.77\,V\ vs.\,SHE \tag{6}$$

The released electrons go through an external circuit and arrive at the cathode. The protons transport through the membrane to the cathode. At the cathode, redox ions (VO_2^{+}) are reduced by receiving the electrons [81]:

$$VO_2^{+} + 2H^{+} + e^{-} \rightarrow VO^{2+} + H_2O \qquad E_a^0 = 1.00\,V\ vs.\,SHE \tag{7}$$

The discharge products, Fe^{3+} ions at the anode and VO^{2+} ions at the cathode, will be chemically charged by ethylene glycol and oxygen in respective reactor according to:

$$\text{Reactor \#1:} \quad HOCH_2CH_2OH + 10Fe^{3+} + 2H_2O \rightarrow 2CO_2 + 10Fe^{2+} + 10H^{+} \tag{8}$$

$$\text{Reactor \#2:} \quad {}^{1}\!/_{2}\,O_2 + 2VO^{2+} + H_2O \rightarrow 2VO_2^{+} + 2H^{+} \tag{9}$$

The combination of Eqs. (7) - (10) results in an overall reaction:

$$HOCH_2CH_2OH + {}^{5}\!/_{2}\,O_2 \rightarrow 2CO_2 + 3H_2O \tag{10}$$

It can be seen that the overall reaction of the present ethylene glycol fuel cell is the same with that of the conventional one. The preliminary results showed that a peak power density of 9.9 mW cm^{-3} (per the volume of graphite felt) was obtained at a voltage of 197 mV, as presented in Fig. 4d. In summary, this ethylene glycol redox fuel cell, which decouples the electrocatalytic oxidation of the ethylene glycol from the electrochemical transfer of electrons to the external circuit, provides several advantages over conventional DEGFCs: (1) this redox fuel cell can realize the almost complete oxidation of ethylene glycol to carbon dioxide (ETR: ~100%), improving the Faraday efficiency; (2) the power output of this fuel cell system depends on the redox couple conversion rate in the electrochemical reactor, potentially yielding a high performance [82]; (3) this fuel cell system avoids all critical issues caused by electrocatalysts in conventional fuel cell systems; and (4) the sole use of carbon materials in preparing the electrodes makes this fuel cell durable. Although promising, the performance needs to be much improved before widespread commercialization becomes possible. Hence, future attention should be paid to the development of membrane materials and optimization of the structural design and operating parameters in order to boost the power output.

5.3. Micro/Nanofluidic fuel cells running on ethylene glycol

Arjona et al. [83] fabricated an alkaline microfluidic fuel cell running on ethylene glycol as fuel and dissolved oxygen as oxidant, as shown in Fig. 5a, in which the Au-Pd supported on polyaniline with a homogeneous semi-spherical shape was used as the anode electrocatalysts. This microfluidic ethylene glycol fuel cell was tested with the anolyte (0.5/1.0/2.0 M ethylene glycol + 0.3 M KOH) and catholyte (dissolved oxygen in 0.3 M KOH) at a flow rate of 11 mL h^{-1} and 3 mL h^{-1}, respectively, at which the fuel cell exhibited stable co-laminar flows and the OCVs were around 0.4 V for 0.5-M ethylene glycol operation and 0.53 V for 1.0- and 2.0-M ethylene glycol operations, respectively, as shown in Fig. 5b.

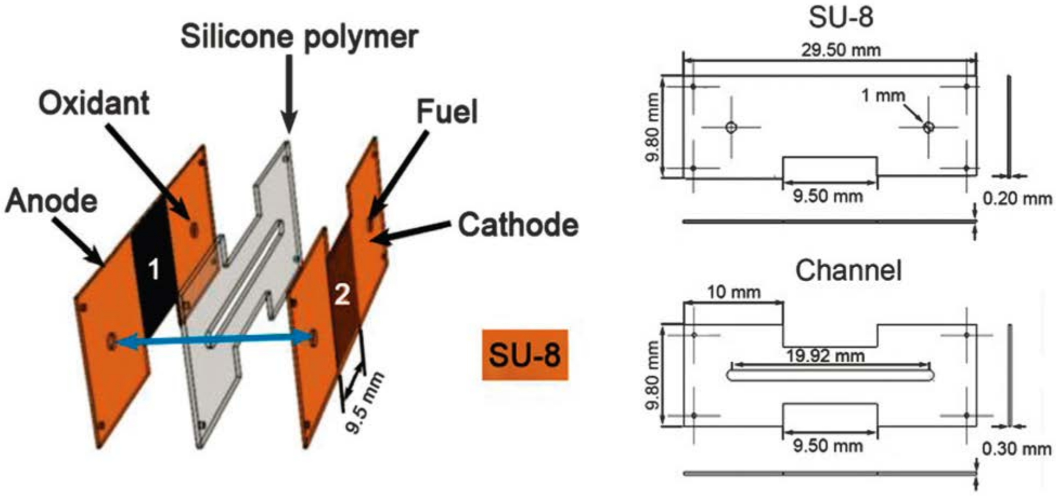

(a)

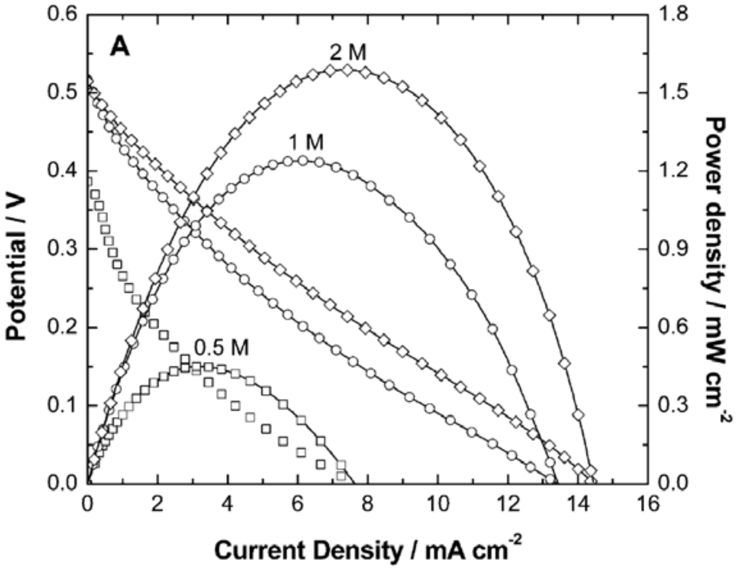

(b)

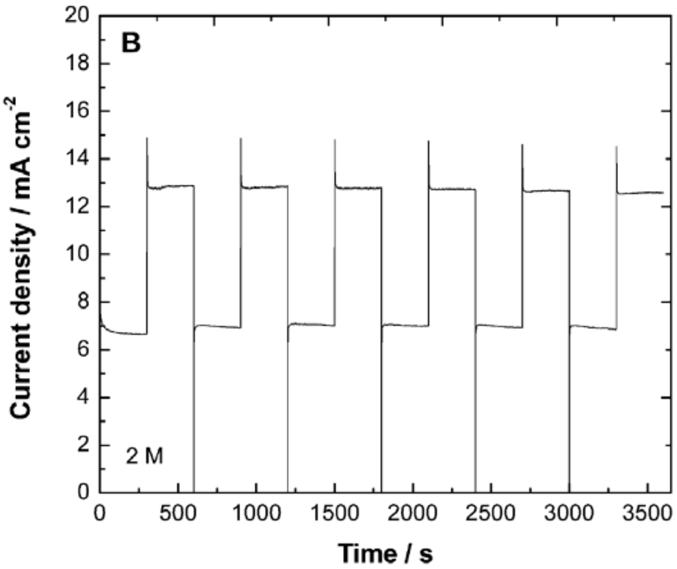

(c)

Fig. 5 (a) Design and dimensions of a microfluidic fuel cell; (b) polarization and power density curves at different ethylene gluycol coencnterations; and (c) stability curves at 0.21 V and 0.02 V [83]. Reproduced with permission from The Royal Society of Chemistry.

The lower OCV at 0.5-M ethylene glycol operation was attributed to the fact that the majority of active surface was occupied by hydroxide ions, lowering the electrochemical kinetics of the ethylene glycol oxidation. In addition, the microfluidic ethylene glycol fuel cell stability was examined with a 2.0-M ethylene glycol at 0.02 V and 0.21 V, as shown in Fig. 5c. They found that the current density remained constant after several cycles. Maya-Cornejo et al. [84] designed and constructed an alkaline membraneless nanofluidic fuel cell with flow-through electrodes, which can run on several fuels (individually or in a mixed manner), such as methanol, ethanol, ethylene glycol and glycerol in an air-breathing mode, as shown in Fig. 6a, in which the Cu-Pd core-shell was used as the anode electrocatalysts.

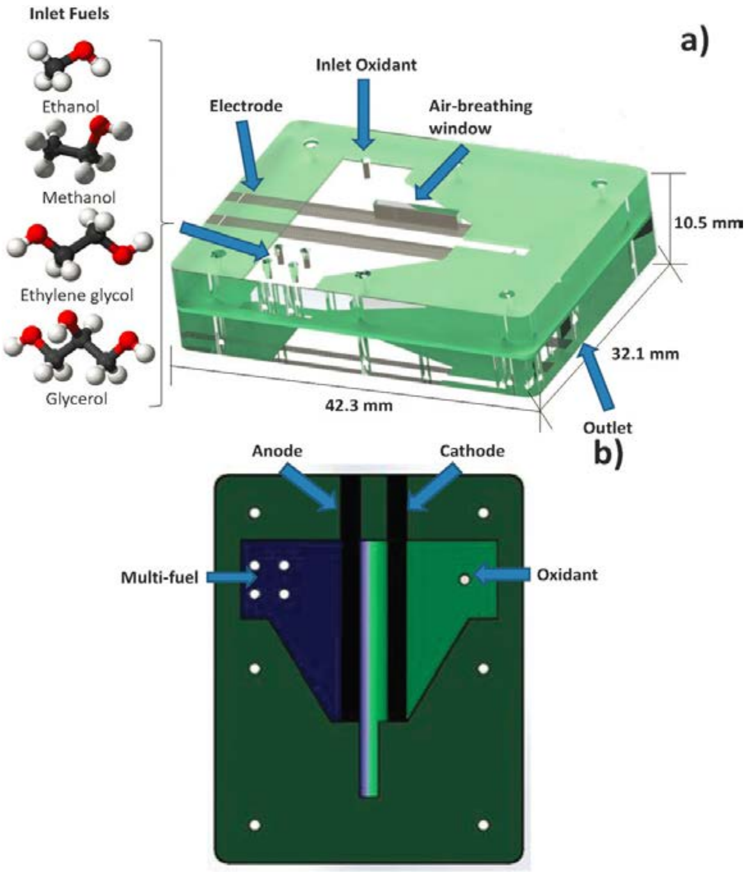

(a)

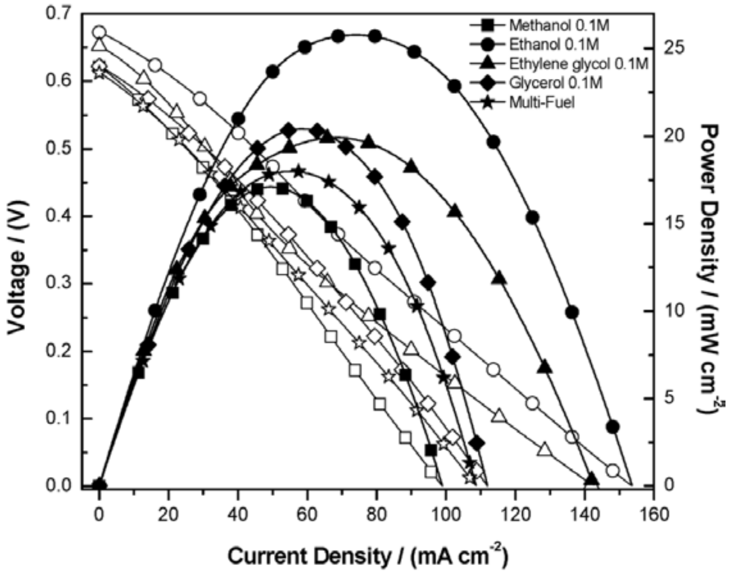

(b)

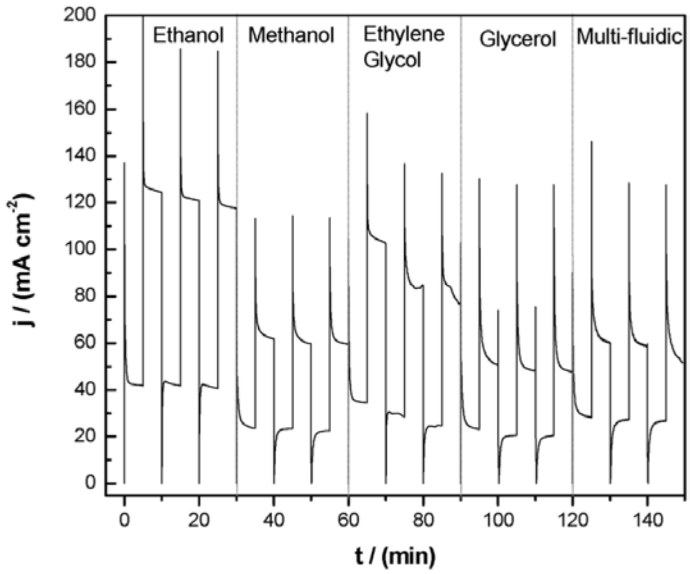

(c)

It was found that when this nanofluidic fuel cell was operated with 0.1 M ethylene glycol (in 0.3 M KOH) at a flow rate of 3 mL h^{-1} and O_2-saturated 0.3 M KOH solution at a flow rate of 6 mL h^{-1}, a peak power density of 19.95 mW cm^{-2} was achieved at room temperature, as shown in Fig. 6b, which is much higher than that yielded by the above-mentioned microfluidic ethylene glycol fuel cell. The performance improvement was attributed to employing the concept of flow-through electrodes with a high active surface area (450 m^2 g^{-1}) of the nanoporous carbon foam and using a combination of dissolved oxygen and air as oxidant. In addition, the nanofluidic fuel cell stability was also examined for a continuous flow of each fuel and the multi-fuel mixture, as shown in Fig. 6c, when the cell was operated with charge and discharge potentials of 0.3 and 0.01 V, respectively. In summary, the previous investigations suggest that the micro/nanofluidic fuel cells running on ethylene glycol have potential applications in micropower devices and electrochemical sensors.

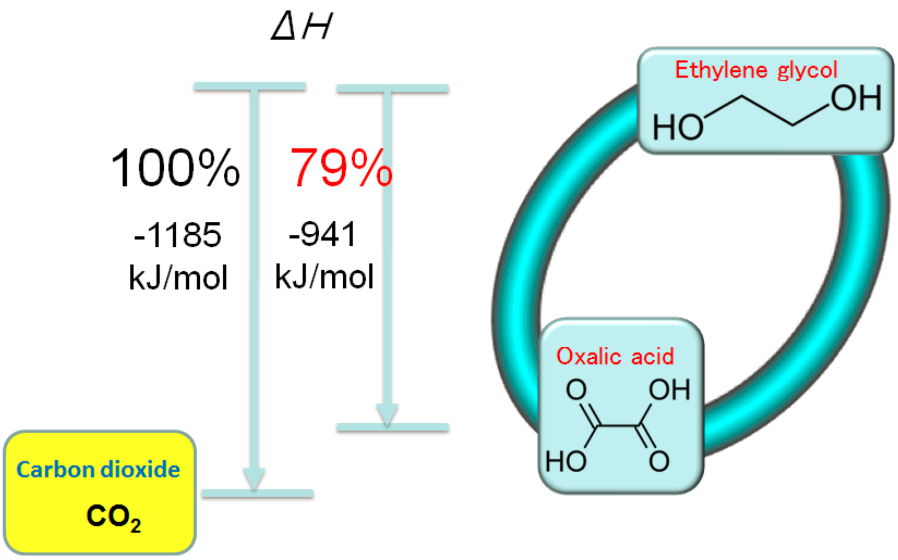

(d)

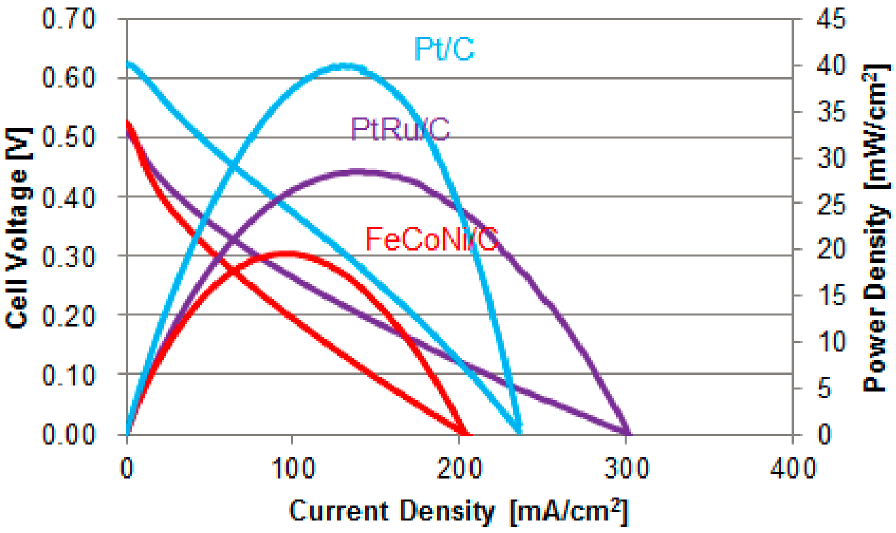

(e)

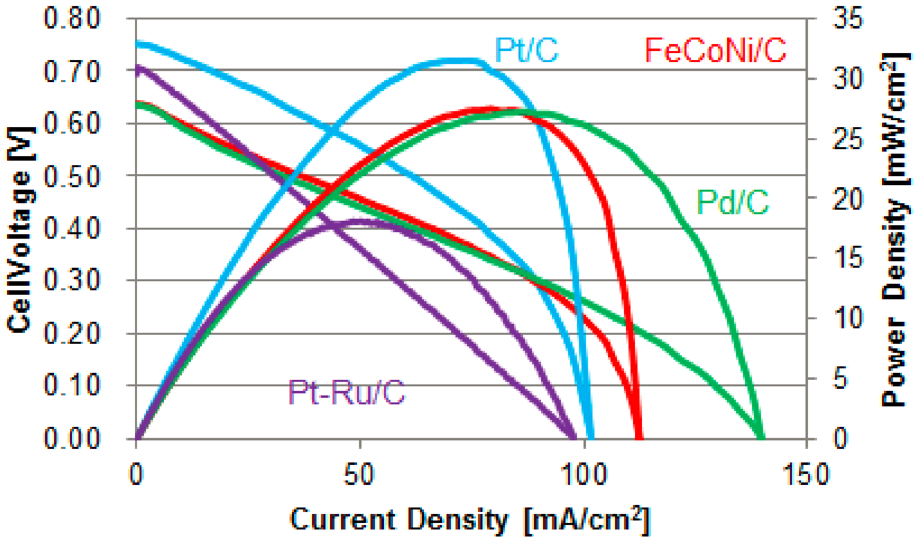

(f)

Fig. 6 (a) Design and dimensions of a nanofluidic fuel cell; (b) polarization and power density curves with various fuels; and (c) stability curves [84]. Reproduced with permission from The Royal Society of Chemistry. (d) A carbon-neutral energy-cycle system using ethylene glycol; (e) and (f) polarization and power density curves of alkaline direct ethylene glycol fuel cells respectively using $NaCo_2O_4$ solid electrolyte and $LaSr_3Fe_3O_{10}$ solid electrolyte [87]. Reproduced with permission from The Electrochemical Society.

5.4. A carbon-neutral energy-cycle system using ethylene glycol as energy carrier

As mentioned earlier, the major product of the ethylene glycol oxidation on the Pd/Pd-based electrocatalysts could be oxalic acid/oxalate due to the high selectivity of the Pd/Pd-based electrocatalysts and the extreme difficulty in breaking the C-C bond of ethylene glycol at low temperatures [85]. On the other hand, it has been demonstrated that it is feasible to convert oxalic acid/oxalate to ethylene glycol via a photocatalytic process [86]. As such, ethylene glycol can be an energy carrier in an energy-storage system via interconversion between ethylene glycol and oxalic acid (oxalate). Takeguchi et al. [87] proposed the concept of carbon-neutral energy-cycle system using ethylene glycol as energy carrier, as illustrated in Figs. 6d-6f. In principle, the power can be generated via an electrocatalytic oxidation of ethylene glycol to oxalic acid (oxalate); and then the solar energy can be stored via a photocatalytic reduction of oxalic acid (oxalate) to ethylene glycol. As shown in Eq. (12) and Eq. (13), the reaction enthalpy of the selective and complete oxidation of ethylene glycol to oxalic acid/oxalate and carbon dioxide, respectively, is -941 kJ/mol and -1185 kJ/mol.

$$HOCH_2 - CH_2OH + {}^5\!/_2 O_2 \rightarrow 2CO_2 + 3H_2O \qquad \Delta_r H = -1185\ kJ/mol \tag{11}$$

or

$$HOCH_2 - CH_2OH + 2O_2 + 2OH^- \rightarrow (COO^-)_2 + 4H_2O\ \Delta_r H = -941\ kJ/mol \tag{12}$$

It is indicated that the released energy via the selective oxidation of ethylene glycol to oxalic acid (oxalate) is 79% of that via the complete oxidation of ethylene glycol to carbon dioxide. In addition, the Gibbs free energy of the selective oxidation reaction of ethylene glycol, $\Delta_r G$, is -845 kJ/mol, resulting in a theoretical energy-conversion efficiency (thermodynamic efficiency) of 90%. Furthermore, they fabricated alkaline

DEGFCs with using Pt/C, Pt-Ru/C, or Fe-Co-Ni/C as the anode electrocatalysts, inorganic materials ($NaCo_2O_4$) as the solid-state electrolyte, and a catalyst-free cathode, which were operated at 70°C with an aqueous solution containing 10 wt.% ethylene glycol + 10 wt.% KOH as fuel and the dry pure oxygen as oxidant. It was found that among three cells, the one using Pt/C as the anode electrocatalysts resulted in the highest OCV of 0.62 V and the highest peak power density of 40 mW cm^{-2} at a current density of 130 mA cm^{-2}. When the solid-state electrolyte was changed from $NaCo_2O_4$ to $LaSr_3Fe_3O_{10}$ and the operating temperature was decreased from 70°C to 40°C, the fuel cell using Pt/C as the anode electrocatalysts showed the highest OCV of 0.75V and the highest peak power density of 32 mW cm^{-2} at a current density of 80 mA cm^{-2}. It should be pointed out that when a non-precious metal catalyst (Fe-Co-Ni/C) was used, the fuel cell resulted in a peak power density of 27 mW cm^{-2} at a current density of 90 mA cm^{-2}. As for the reduction of oxalic acid/oxalate, they proposed a potential approach, i.e., photocatalytic process, to close the renewable energy-storage system. In addition, the reduction of oxalic acid/oxalate to ethylene glycol can also be achieved via an electrochemical method [21].

6. Concluding remarks

This review gives an overview of the past investigations on alkaline direct ethylene glycol fuel cells, in terms of the physical and chemical processes through the fuel cell structure, the oxidation of ethylene glycol on metal electrodes, the electrocatalysts toward the ethylene glycol oxidation, as well as the singe-cell performance. In addition, four innovative fuel-cell system designs are also highlighted, including solid oxide fuel cells, redox fuel cells, micro/nanofluidic fuel cells, as well as a renewable energy-storage system, all of which are running on ethylene glycol. Although promising, the power output of alkaline DEGFCs have to be substantially increased before widespread application becomes possible. Such improvement depends on finding solutions to the following critical issues: (1) the most important and challenging issue is how to achieve a direct 10-electron electrocatalytic oxidation of ethylene glycol to carbon dioxide; (2) the electrode design must be optimized, which critically depends on a clear understanding of transport phenomena through the multi-layered structure; (3) the effects of the liquid electrolyte on the existing electrocatalytic and membrane materials during a long-term operation also need to be addressed; and (4) a scientifically sound numerical approach for designing and optimizing alkaline direct ethylene glycol fuel cells should be developed to guide future efforts.

Acknowledgements

The authors gratefully acknowledge the financial supports of the Natural Science Foundation of China (No. 51506039 and No. 51576021).

References

[1] S.P.S. Badwal, S. Giddey, A. Kulkarni, J. Goel, S. Basu, Direct ethanol fuel cells for transport and stationary applications-A comprehensive review, Applied Energy 145 (2015) 80-103.

[2] L. An, T.S. Zhao, S.Y. Shen, Q.X. Wu, R. Chen, An alkaline direct oxidation fuel cell with non-platinum catalysts capable of converting glucose to electricity at high power output, J. Power Sources 196 (2011) 186-190.

[3] A. Brouzgou, A. Podias, P. Tsiakaras, PEMFCs and AEMFCs directly fed with ethanol: a current status comparative review, J. Appl Electrochem 43 (2013) 119-136.

[4] L. An, T.S. Zhao, X.H. Yan, X.L. Zhou, P. Tan, The dual role of hydrogen peroxide in fuel cells, Science Bulletin 60 (2015) 55-64.

[5] J. Ma, N.A. Choudhury, Y. Sahai, A comprehensive review of direct borohydride fuel cells, Renewable and Sustainable Energy Reviews 14 (2010) 183-199.

[6] L. An, T.S. Zhao, Y.S. Li, Carbon-neutral sustainable energy technology: Direct ethanol fuel cells, Renewable and Sustainable Energy Reviews 50 (2015) 1462-1468.

[7] L. An, T.S. Zhao, L. Zeng, X.H. Yan, Performance of an alkaline direct ethanol fuel cell with hydrogen peroxide as oxidant, Int. J. Hydrogen Energy 39 (2014) 2320-2324.

[8] L. An, T.S. Zhao, Y.S. Li, Q.X. Wu, Charge carriers in alkaline direct oxidation fuel cells, Energy & Environmental Science 5 (2012) 7536-7538.

[9] L. An, T.S. Zhao, R. Chen, Q.X. Wu, A novel direct ethanol fuel cell with high power density, J. Power Sources 196 (2011) 6219–6222.

[10] L. An, T.S. Zhao, Performance of an alkaline-acid direct ethanol fuel cell, Int. J. Hydrogen Energy 36 (2011) 9994-9999.

[11] L. An, T.S. Zhao, J.B. Xu, A bi-functional cathode structure for alkaline-acid direct ethanol fuel cells, Int. J. Hydrogen Energy 36 (2011) 13089-13095.

[12] L. An, Z.H. Chai, L. Zeng, P. Tan, T.S. Zhao, Mathematical modeling of alkaline direct ethanol fuel cells, Int. J. Hydrogen Energy 38 (2013) 14067 -14075.

[13] E. Antolini, E.R. Gonzalez, Alkaline direct alcohol fuel cells, J. Power Sources 195 (2010) 3431-3450.

[14] C. Bianchini, P.K. Shen, Palladium-based electrocatalysts for alcohol oxidation in half cells and in direct alcohol fuel cells, Chem. Rev. 109 (2009) 4183-4206.

[15] H.R. Yue, Y.J. Zhao, X.B. Ma, J.L. Gong, Ethylene glycol properties, synthesis, and applications, Chem. Soc. Rev. 41 (2012) 4218-4244.

[16] C. Cremers, A. Niedergesäß, F. Jung, D. Müller, J. Tübke, Development of an alkaline anion exchange membrane direct ethylene glycol fuel cell stack, ECS Transactions 41 (2011) 1987-1996.

[17] E. Antolini, Palladium in fuel cell catalysis, Energy Environ. Sci. 2 (2009) 915-931.

[18] Z. Ogumi, K. Matsuoka, S. Chiba, M. Matsuoka, Y. Iriyama, T. Abe, M. Inaba, Prelimimnary study on direct alcohol fuel cells employing anion exchange membrane, Electrochemistry 70 (2002) 980-983.

[19] E.H. Yu, X. Wang, U. Krewer, l. Li, K. Scott, Direct oxidation alkaline fuel cells from materials to systems, Energy Environ. Sci. 5 (2012) 5668-5680.

[20] A. Serov, C. Kwak, Recent achievements in direct ethylene glycol fuel cells (DEGFC), Applied Catalysis B: Environmental 97 (2010) 1-12.

[21] S.C. Ma, M. Sadakiyo, R. Luo, M. Heima, M. Yamauchi, P.J.A. Kenis, One-step electrosynthesis of ethylene and ethanol from CO_2 in an alkaline electrolyzer, J. Power Sources 301 (2016) 219-228.

[22] M.Y. Zheng, A.Q. Wang, N. Ji, J.F. Peng, X.D. Wang, T. Zhang, Transition metal-tungsten bimetallic catalysts for the conversion of cellulose into ethylene glycol, ChemSusChem 3 (2010) 63-66.

[23] D. Bayer, S. Berenger, M. Joos, C. Cremers, J. Tübke, Electrochemical oxidation of C_2 alcohols at platinum electrodes in acidic and alkaline environment, Int. J. Hydrogen Energy 35 (2010) 12660-12667.

[24] S.W. Xie, S. Chen, Z.Q. Liu, C.W. Xu, Comparison of alcohol electrooxidation

on Pt and Pd Electrodes in alkaline medium, Int. J. Electrochem. Sci. 6 (2011) 882-888.

[25] K. Matsuoka, M. Inaba, Y. Iriyama, T. Abe, Z. Ogumi, M. Matsuoka, Anodic oxidation of polyhydric alcohols on a Pt Electrode in alkaline solution, Fuel Cells 2 (2002) 35-39.

[26] K. Matsuoka, Y. Iriyama, T. Abe, M. Matsuoka, Z. Ogumi, Electro-oxidation of methanol and ethylene glycol on platinum in alkaline solution: Poisoning effects and product analysis, Electrochimica Acta 51 (2005) 1085-1090.

[27] P.A. Christensen, A. Hamnett, The oxidation of ethylene glycol at a platinum electrode in acid and base: An in situ FTIR study, J. Electroanal. Chem. 260 (1989) 347-359.

[28] S.C. Chang, Y. Ho, M.J. Weaver, Applications of real-time FTIR spectroscopy to the elucidation of complex electroorganic pathways electrooxidation of ethylene glycol on gold, platinum, and nickel in alkaline solution, J. Am. Chem. Soc. 113 (1991) 9506-9513.

[29] F. Hahn, B. Beden, F. Kadirgan, C. Lamy, Electrocatalytic oxidation of ethylene glycol Part III. In-situ infrared reflectance spectroscopic study of the strongly bound species resulting from its chemisorption at a platinum electrode in aqueous medium, J. Electroanal. Chem. 216 (1987) 169-180.

[30] E. Sitta, B.C. Batista, H. Varela, The impact of the alkali cation on the mechanism of the electro-oxidation of ethylene glycol on Pt, Chem. Commun. 47 (2011) 3775-3777.

[31] C.A. Angelucci, H. Varela, G. Tremiliosi-Filho, J.F. Gomes, The significance of non-covalent interactions on the electro-oxidation of alcohols on Pt and Au in alkaline media, Electrochemistry Communications 33 (2013) 10-13.

[32] E. Sitta, H. Varela, Beta oscillations in the electro-oxidation of ethylene glycol on platinum, Electrocatalysis 1 (2010) 19-21.

[33] E. Sitta, M.A. Nascimento, H. Varela, Complex kinetics, high frequency oscillations and temperature compensation in the electro-oxidation of ethylene glycol on platinum, Phys. Chem. Chem. Phys. 12 (2010) 15195-15206.

[34] K. Matsuoka, Y. Iriyama, T. Abe, M. Matsuoka, Z. Ogumi, Electrocatalytic oxidation of ethylene glycol in alkaline solution, J. The Electrochemical Society 152 (2005) A729-A731.

[35] L. Demarconnay, S. Brimaud, C. Coutanceau, J.M. Léger, Ethylene glycol electrooxidation in alkaline medium at multi-metallic Pt based catalysts, J. Electroanalytical Chemistry 601 (2007) 169-180.

[36] C. Coutanceau, L. Demarconnay, C. Lamy, J.M. Léger, Development of electrocatalysts for solid alkaline fuel cell (SAFC), J. Power Sources 156 (2006)

14-19.

[37] F. Kadirgan, B. Beden, C. Lamy, Electrocatalytic oxidation of ethylene-glycol Part II. Behaviour of platinum-ad-atom electrodes in alkaline medium, J. Electroanal. Chem. 143 (1983) 135-152.

[38] N.W. Smimova, O.A. Petrii, Effect of ad-atoms on the electro-oxidation of ethylene glycol and oxalic acid on platinized platinum, J. Electroanal. Chem. 251 (1988) 73-87.

[39] N. Dalbay, F. Kadirgan, Electrolytically co-deposited platinum-palladium electrodes and their electrocatalytic activity for ethylene glycol oxidation a synergistic effect, Electrochimica Acta 36 (1991) 353-356.

[40] L.Q. Wang, H. Meng, P.K. Shen, C. Bianchini, F. Vizza, Z.D. Wei, In situ FTIR spectroelectrochemical study on the mechanism of ethylene glycol electrocatalytic oxidation at a Pd electrode, Phys. Chem. Chem. Phys. 13 (2011) 2667-2673.

[41] V. Bambagioni, M. Bevilacqua, C. Bianchini, J. Filippi, A. Lavacchi, A. Marchionni, F. Vizza, P.K. Shen, Self-sustainable production of hydrogen, chemicals, and energy from renewable alcohols by electrocatalysis, ChemSusChem 3 (2010) 851-855.

[42] T. Matsumoto, M. Sadakiyo, M.L. Ooi, S. Kitano, T. Yamamoto, S. Matsumura, K. Kato, T. Takeguchi, M. Yamauchi, CO_2-free power generation on an iron group

nanoalloy catalyst via selective oxidation of ethylene glycol to oxalic acid in alkaline media, Scientific Reports 4 (2014) 1-6.

[43] T. Matsumoto, M. Sadakiyo, M.L. Ooi, T. Yamamoto, S. Matsumura, K. Kato, T. Takeguchi, N. Ozawa, M. Kubo, M. Yamauchi, Atomically mixed Fe-group nanoalloys catalyst design for the selective electrooxidation of ethylene glycol to oxalic acid, Phys. Chem. Chem. Phys. 17 (2015) 11359-11366.

[44] V. Bambagioni, M. Bevilacqua, C. Bianchini, J. Filippi, A. Marchionni, F. Vizza, L.Q.Wang, P.K. Shen, Ethylene glycol electrooxidation on smooth and nanostructured Pd electrodes in alkaline media, Fuel Cells 10 (2010) 582-590.

[45] J.L. Lin, J. Ren, N. Tian, Z.Y. Zhou, S.G. Sun, In situ FTIR spectroscopic studies of ethylene glycol electrooxidation on Pd electrode in alkaline solution The effects of concentration, J. Electroanalytical Chemistry 688 (2013) 165-171.

[46] B. Beden, I. Cetin, A. Kahyaoglu, D. Takky, C. Lamy, lectrocatalytic oxidation of saturated oxygenated compounds on gold electrodes, J. Catalysis 104 (1987) 37-46.

[47] M.S. Ureta-Zañartu, A. Alarcón, G. Muñoz, C. Gutiérrez, Electrooxidation of methanol and ethylene glycol on gold and on gold modified with an electrodeposited polyNiTSPc film, Electrochimica Acta 52 (2007) 7857-7864.

[48] R.R. Adzic, M. Avramov-Ivic, Structural effects in electrocatalysis Oxidation of ethylene glycol on single crystal gold electrodes in alkaline solutions, J. Catalysis 101

(1986) 532-535.

[49] D. Pletcher, M. Fleischmann, K. Korinek, The oxidation of organic compounds at a cobalt electrode in alkaline media, J. Electroanal. Chem. 33 (1971) 478-479.

[50] L. Xin, Z.Y. Zhang, J. Qi, D. Chadderdon, W.Z. Li, Electrocatalytic oxidation of ethylene glycol (EG) on supported Pt and Au catalysts in alkaline media Reaction pathway investigation in three-electrode cell and fuel cell reactors, Applied Catalysis B: Environmental 125 (2012) 85-94.

[51] Y. Kim, H. Kim, W.B. Kim, PtAg nanotubes for electrooxidation of ethylene glycol and glycerol in alkaline media, Electrochemistry Communications 46 (2014) 36-39.

[52] C.W. Xu, P.K. Shen, Novel Pt/CeO_2/C catalysts for electrooxidation of alcohols in alkaline media, Chem. Commun. (2004) 2238-2239.

[53] C.W. Xu, R. Zeng, P.K. Shen, Z.D. Wei, Synergistic effect of CeO_2 modified Pt/C catalysts on the alcohols oxidation, Electrochimica Acta 51 (2005) 1031-1035.

[54] R. Pattabiraman, Electrochemical investigations on carbon supported palladium catalysts, Applied Catalysis A: General 153 (1997) 9-20.

[55] S.S. Li, Y.Y. Hu, J.J. Feng, Z.Y. Lv, J.R. Chen, A.J. Wang, Rapid room-temperature synthesis of Pd nanodendrites on reduced graphene oxide for catalytic oxidation of ethylene glycol and glycerol, Int. J. Hydrogen Energy 39 (2014)

3730-3738.

[56] S. Cherevko, N. Kulyk, C.H. Chung, Nanoporous palladium with sub-10 nm dendrites by electrodeposition for ethanol and ethylene glycol oxidation, Nanoscale 4 (2012) 103-105.

[57] C.W. Xu, Y.L. Liu, D.S. Yuan, Pt and Pd supported on carbon microspheres for alcohol electrooxidation in alkaline media, Int. J. Electrochem. Sci. 2 (2007) 674-680.

[58] T. Ramulifho, K.I. Ozoemena, R.M. Modibedi, C.J. Jafta, M.K. Mathe, Electrocatalytic oxidation of ethylene glycol at palladium-bimetallic nanocatalysts (PdSn and PdNi) supported on sulfonate-functionalised multi-walled carbon nanotubes, J. Electroanalytical Chemistry 692 (2013) 26-30.

[59] A. Serov, U. Martinez, P. Atanassov, Novel Pd-In catalysts for alcohols electrooxidation in alkaline media, Electrochemistry Communications 34 (2013) 185-188.

[60] R. Kannan, K. Karunakaran, S. Vasanthkumar, PdNi-decorated manganite nanocatalyst for electrooxidation of ethylene glycol in alkaline media, Ionics 18 (2012) 803-809.

[61] A. Marchionni, M. Bevilacqua, C. Bianchini, Y.X. Chen, J. Filippi, P. Fornasiero, A. Lavacchi, H. Miller, L.Q. Wang, F. Vizza, Electrooxidation of ethylene glycol and glycerol on Pd-(Ni-Zn)/C anodes in direct alcohol fuel cells, ChemSusChem 6 (2013)

518-528.

[62] O.O. Fashedemi, K.I. Ozoemena, Comparative electrocatalytic oxidation of ethanol, ethylene glycol and glycerol in alkaline medium at Pd-decorated FeCo@FeC core-shell nanocatalysts, Electrochimica Acta 128 (2014) 279-286.

[63] O.O. Fashedemi, H.A. Miller, A. Marchionni, F. Vizza, K.I. Ozoemena, Electro-oxidation of ethylene glycol and glycerol at palladium-decorated FeCo@Fe core-shell nanocatalysts for alkaline direct alcohol fuel cells functionalized MWCNT supports and impact on product selectivity, J. Mater. Chem. A 3 (2015) 7145-7156.

[64] P.K. Shen, C.W. Xu, Alcohol oxidation on nanocrystalline oxide Pd/C promoted electrocatalysts, Electrochemistry Communications 8 (2006) 184-188.

[65] C.W. Xu, Z.Q. Tian, P.K. Shen, S.P. Jiang, Oxide (CeO_2, NiO, Co_3O_4 and Mn_3O_4)-promoted Pd/C electrocatalysts for alcohol electrooxidation in alkaline media, Electrochimica Acta 53 (2008) 2610-2618.

[66] S. Yongprapat, A.Therdthianwong, S.Therdthianwong, Au/C catalysts promoted with metal oxides for ethylene glycol electro-oxidation in alkaline solution, J. Electroanalytical Chemistry 697 (2013) 46-52.

[67] L. Xin, Z.Y. Zhang, J. Qi, D. Chadderdon, W.Z. Li, Electrocatalytic oxidation of ethylene glycol (EG) on supported Pt and Au catalysts in alkaline media Reaction pathway investigation in three-electrode cell and fuel cell reactors, Applied Catalysis

B: Environmental 125 (2012) 85-94.

[68] C.C. Jin, Y.S. Song, Z.D. Chen, A comparative study of the electrocatalytic oxidation of ethylene glycol on PtAu nanocomposite catalysts in alkaline, neutral and acidic media, Electrochimica Acta 54 (2009) 4136-4140.

[69] M. Brandalise, M.M. Tusi, R.M. Piasentin, M.C. Santos, E.V. Spinacé, A.O. Neto, Synthesis of PdAu/C and PdAuBi/C electrocatalysts by borohydride reduction method for ethylene glycol electrooxidation in alkaline medium, Int. J. Electrochem. Sci. 7 (2012) 9609-9621.

[70] H. Ewe, E. Just, M. Pesditschek, Ethylene glycol as fuel for alkaline fuel cells, Energy Conversion. 15 (1975) 9-14.

[71] L. An, R. Chen, Direct formate fuel cells: A review, J. Power Sources 320 (2016) 127-139.

[72] K. Matsuoka, Y. Iriyama, T. Abe, M. Matsuoka, Z. Ogumi, Alkaline direct alcohol fuel cells using an anion exchange membrane, J. Power Sources 150 (2005) 27-31.

[73] L. An, T.S. Zhao, S.Y. Shen, Q.X. Wu, R. Chen, Performance of a direct ethylene glycol fuel cell with an anion-exchange membrane, Int. J. Hydrogen Energy 35 (2010) 4329-4335.

[74] L. An, L. Zeng, T.S. Zhao, An alkaline direct ethylene glycol fuel cell with an

alkali-doped polybenzimidazole membrane, Int. J. Hydrogen Energy 38 (2013) 10602-10606.

[75] J.R. Varcoe, R.C.T. Slade, Prospects for alkaline anion-exchange membranes in low temperature fuel cells, Fuel Cells 5 (2005) 187-200.

[76] J.R. Varcoe, P. Atanassov, D.R. Dekel, A.M. Herring, M.A. Hickner, P.A. Kohl, A.R. Kucernak, W.E. Mustain, K. Nijmeijer, K. Scott, T.W. Xu, L. Zhuang, Anion-exchange membranes for electrochemical energy systems, Energy Environ. Sci. 7 (2014) 3135-3191.

[77] J.R. Varcoe, R.C.T. Slade, E.L.H. Yee, S.D. Poynton, D.J. Driscoll, Investigations into the ex situ methanol, ethanol and ethylene glycol permeabilities of alkaline polymer electrolyte membranes, J. Power Sources 173 (2007) 194-199.

[78] J.F. Qu, W. Wang, Y.B. Chen, F. Wang, R. Ran, Z.P. Shao, Ethylene glycol as a new sustainable fuel for solid oxide fuel cells with conventional nickel-based anodes, Applied Energy 148 (2015) 1-9.

[79] C.B. Gorman, S.H. Bergens, G.M. Whitesides, Platinum-catalyzed oxidations of organic compounds by ferric sulfate use of a redox fuel cell to mediate complete oxidation of EG by dioxygen at 80^{o}C, J. Catalysis 158 (1996) 92-96.

[80] Y.K. Zeng, T.S. Zhao, L. An, X.L. Zhou, L. Wei, A comparative study of all-vanadium and iron-chromium redox flow batteries for large-scale energy storage, J.

Power Sources 300 (2015) 438-443.

[81] L. An, T.S. Zhao, X.L. Zhou, X.H. Yan, C.Y. Jung, A low-cost, high-performance zinc-hydrogen peroxide fuel cell, J. Power Sources 275 (2015) 831-834.

[82] L. An, T.S. Zhao, X.L. Zhou, L. Wei, X.H. Yan, A high-performance ethanol-hydrogen peroxide fuel cell, RSC Advances 4 (2014) 65031-65034.

[83] N. Arjona, A. Palacios, A. Moreno-Zuria, M. Guerra-Balcázar, J. Ledesma-García, L.G. Arriaga, AuPd/polyaniline as the anode in an ethylene glycol microfluidic fuel cell operated at room temperature, Chem. Commun. 50 (2014) 8151-8153.

[84] J. Maya-Cornejo, E. Ortiz-Ortega, L. Álvarez-Contreras, N. Arjona, M. Guerra-Balcázar, J. Ledesma-García, L.G. Arriaga, Copper–palladium core–shell as an anode in a multi-fuel membraneless nanofluidic fuel cell toward a new era of small energy conversion devices, Chem. Commun. 51 (2015) 2536-2539.

[85] F. Munoz, C. Hua, T. Kwong, L. Tran, T.Q. Nguyen, J.L. Haan, Palladium–copper electrocatalyst for the promotion of the electrochemical oxidation of polyalcohol fuels in the alkaline direct alcohol fuel cell, Applied Catalysis B: Environmental 174-175 (2015) 323-328.

[86] S.C. Roy, O.K. Varghese, M. Paulose, C.A. Grimes, Toward solar fuels: Photocatalytic conversion of carbon dioxide to hydrocarbons, ACS Nano, 4 (2010)

1259-1278.

[87] T. Takeguchi, H. Arikawa, M. Yamauchi, R. Abe, Selective ethylene glycol oxidation reaction for carbon neutral energy cycle system, ECS Transactions 41 (2011) 1755-1759.

Table captions:

Table 1 The pathways of ethylene glycol electro-oxidation on a Pd electrode at different pH values [40].

Table 2 Selected alkaline direct ethylene glycol fuel cell performance reported in the literature.

Figure captions:

Fig. 1 (a) Reaction pathways of ethylene glycol electro-oxidation in alkaline media [26]. Reproduced with permission from Elsevier. (b) Reaction pathway of ethylene glycol electro-oxidation on a Pd electrode in alkaline media [40]. Reproduced with permission from The Royal Society of Chemistry.

Fig. 2 (a) Cyclic voltammograms of ethylene glycol electro-oxidation on Pd-(Ni-Zn)/C (•) and Pd/C (■) electrodes and (b) polarization and power density curves for direct ethylene glycol fuel cells using Pd-(Ni-Zn)/C (○) and Pd/C (•) as anode electrocatalysts at 80°C [61]. Reproduced with permission from Wiley.

Fig. 3 (a) Schematic of a direct alkaline fuel cell using an anion exchange membrane; (b) polarization and (c) power density curves of alkaline direct alcohol fuel cells using polyhydric alcohols at 50°C [72]; (d) schematic of various types of direct ethylene glycol fuel cell; (e) polarization and power density curves at 60°C and 90°C; and (f) constant-current discharging behavior at 90°C [74]. Reproduced with permission from Elsevier.

Fig. 4 Polarization and power density curves of solid oxide fuel cells at different temperatures running on: (a) hydrogen and (b) ethylene glycol steam [78]; (c) schematic of a redox fuel cell running on ethylene glycol and (d) polarization curvres and electrode potentials [79]. Reproduced with permission from Elsevier.

Fig. 5 (a) Design and dimensions of a microfluidic fuel cell; (b) polarization and power density curves at different ethylene gluycol coencnterations; and (c) stability curves at 0.21 V and 0.02 V [83]. Reproduced with permission from The Royal Society of Chemistry.

Fig. 6 (a) Design and dimensions of a nanofluidic fuel cell; (b) polarization and power density curves with various fuels; and (c) stability curves [84]. Reproduced with permission from The Royal Society of Chemistry. (d) A carbon-neutral energy-cycle system using ethylene glycol; (e) and (f) polarization and power density curves of alkaline direct ethylene glycol fuel cells respectively using $NaCo_2O_4$ solid electrolyte and $LaSr_3Fe_3O_{10}$ solid electrolyte [87]. Reproduced with permission from The Electrochemical Society.

pH	Pathway of ethylene glycol electro-oxidation
0-7	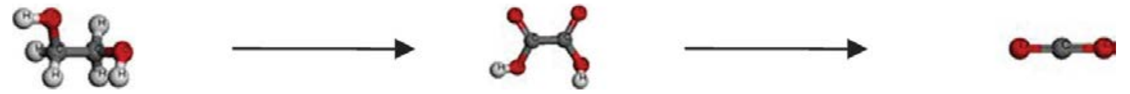
7-13	
13-14.5	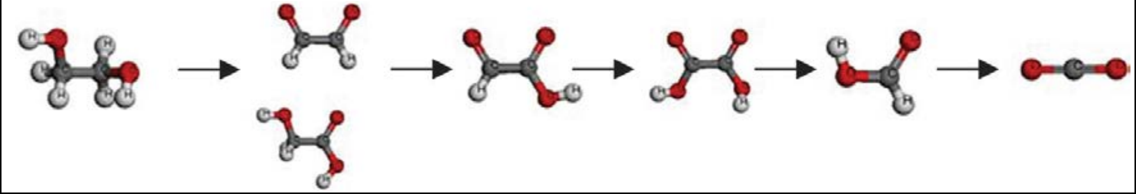
>14.5	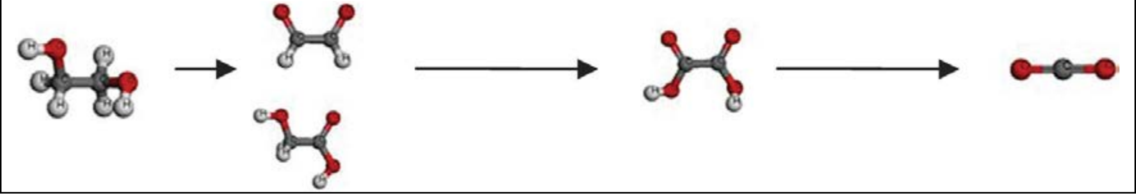

Table 1 The pathways of ethylene glycol electro-oxidation on Pd at different pH values [40]. Reproduced with permission from The Royal Society of Chemistry.

Fuel/Oxidant	**Anode**	**Cathode**	**Membrane**	**T (ºC)**	**PPD (mW cm^{-2})**	**Ref.**
2 mL min^{-1} 2 M EG + 1 M NaOH / 20 sccm O_2	Pt/C 40% (2 mg cm^{-2})	Pt/C 40% (2 mg cm^{-2})	ADP-Morgane®	20	~4	[35]
2 mL min^{-1} 2 M EG + 2 M NaOH / 20 sccm O_2	Pt/C 40% (2 mg cm^{-2})	Pt/C 40% (2 mg cm^{-2})	ADP-Morgane®	20	~13	[35]
2 mL min^{-1} 2 M EG + 4 M NaOH / 20 sccm O_2	Pt/C 40% (2 mg cm^{-2})	Pt/C 40% (2 mg cm^{-2})	ADP-Morgane®	20	19	[35]
2 mL min^{-1} 2 M EG + 4 M NaOH / 20 sccm O_2	Pt/C 20% (2 mg cm^{-2})	Pt/C 40% (2 mg cm^{-2})	ADP-Morgane®	20	8	[35]
2 mL min^{-1} 2 M EG + 4 M NaOH / 20 sccm O_2	Pd/C 20% (2 mg cm^{-2})	Pt/C 40% (2 mg cm^{-2})	ADP-Morgane®	20	~14	[35]
2 mL min^{-1} 2 M EG + 4 M NaOH / 20 sccm O_2	$Pt_{0.9}Bi_{0.1}/C$ 50% (2 mg cm^{-2})	Pt/C 40% (2 mg cm^{-2})	ADP-Morgane®	20	22	[35]
2 mL min^{-1} 2 M EG + 4 M NaOH / 20 sccm O_2	$Pt_{0.45}Pd_{0.45}Bi_{0.1}/C$ 50% (2 mg cm^{-2})	Pt/C 40% (2 mg cm^{-2})	ADP-Morgane®	20	28	[35]
2 M EG +4 M NaOH / O_2	Pt/C (2 mg cm^{-2})	Pt/C (2 mg cm^{-2})	ADP-Morgane®	20	19	[36]
2 mL min^{-1} 2 M EG + 4 M NaOH / 20 sccm O_2	Pt/C (2 mg cm^{-2})	$Pt_{0.8}Bi_{0.2}/C$ (2 mg cm^{-2})	ADP-Morgane®	20	23.5	[88]
2 mL min^{-1} 2 M EG + 4 M NaOH / 20 sccm O_2	Pt/C (2 mg cm^{-2})	Pt/C (2 mg cm^{-2})	ADP-Morgane®	20	19	[88]
2 M KOH + 5 wt % EG / O_2	Pd-(Ni-Zn)/C (1 mg cm^{-2})	Fe-Co/C (1 mg cm^{-2})	Tokuyama A201	25	24	[61]
2 M KOH + 5 wt % EG / O_2	Pd/C (1 mg cm^{-2})	Fe-Co/C (1 mg cm^{-2})	Tokuyama A201	25	12	[61]
2 mL min^{-1} 5 wt% EG + 10 wt% KOH /200 mL min^{-1} air	Hypermec® 3020	Hypermec® 4014	Fumatech fumaPEM A alkaline membrane	50	~7.2	[16]
1.5 mL min^{-1} 5 wt% EG + 10 wt% KOH /200 mL min^{-1} air	Hypermec® 3020	Hypermec® 4014	Fumatech fumaPEM A alkaline membrane	50	~6.5	[16]
2 mL min^{-1} 5 wt% EG + 10 wt% KOH /200 mL min^{-1} air	Hypermec® 3020	Hypermec® 4014	Fumatech fumaSEP FAA membrane	50	~12.6	[16]

2 mL min^{-1} 5 wt% EG + 10 wt% KOH /250 mL min^{-1} air	Hypermec® 3020	Hypermec® 4014	Fumatech fumaPEM FAA2 membrane	50	~45	[16]
1 M EG + 1 M KOH / O$_2$	Pt/C (5 mg cm^{-2})	Pt/C (1 mg cm^{-2})	Tokuyama AHA	50	9.2	[18]
4 mL min^{-1} 1 M EG + 2 M KOH / 400 sccm O$_2$	Pt/C (1 mg cm^{-2})	Fe-Cu-N$_4$/C (Acta 4020) (1 mg cm^{-2})	Tokuyama A201	50	75	[67]
4 mL min^{-1} 0.11 M EG + 2 M KOH / 400 sccm O$_2$	Pt/C (1 mg cm^{-2})	Fe-Cu-N$_4$/C (Acta 4020) (1 mg cm^{-2})	Tokuyama A201	50	25	[67]
4 mL min^{-1} 1 M EG + 2 M KOH / 400 sccm O$_2$	Au/C (1 mg cm^{-2})	Fe-Cu-N$_4$/C (Acta 4020) (1 mg cm^{-2})	Tokuyama A201	50	7.3	[67]
4 mL min^{-1} 0.1 M EG + 2 M KOH / 400 sccm O$_2$	Au/C (1 mg cm^{-2})	Fe-Cu-N$_4$/C (Acta 4020) (1 mg cm^{-2})	Tokuyama A201	50	1.3	[67]
50 mL min^{-1} 1 M EG + 1 M KOH / 50 sccm O$_2$ (humidified)	Pt-Ru/C (4 mg cm^{-2})	Pt/C (1 mg cm^{-2})	Tokuyama AHA	50	9.8	[72]
50 mL min^{-1} 3 M EG + 1 M KOH / 50 sccm O$_2$ (humidified)	Pt-Ru/C (4 mg cm^{-2})	Pt/C (1 mg cm^{-2})	Tokuyama AHA	50	8.1	[72]
50 mL min^{-1} 5 M EG + 1 M KOH / 50 sccm O$_2$ (humidified)	Pt-Ru/C (4 mg cm^{-2})	Pt/C (1 mg cm^{-2})	Tokuyama AHA	50	7.4	[72]
10 mL min^{-1} 2 M EG / 2000 sccm humidified O$_2$ (RH=100%)	Pt:Ru (1:1)/C (4 mg cm^{-2})	Pt/C (4 mg cm^{-2})	ETFE-based radiation-grafted alkaline anion exchange membrane	50	~1.8	[77]
10 mL min^{-1} 2 M EG / 2000 sccm humidified O$_2$ (RH=100%)	Pt:Ru (1:1)/C (4 mg cm^{-2})	Pt/C (4 mg cm^{-2})	Cross-lined alkaline anion exchange membrane	50	~1.6	[77]
2 mL min^{-1} 5 wt% EG + 10 wt% KOH /200 mL min^{-1} air	Hypermec® 3020	Hypermec® 4014	Fumatech fumaPEM A alkaline membrane	60	~8.0	[16]
2 mL min^{-1} 1 M EG + 7 M KOH / 100 sccm O$_2$	PdNi/C (2 mg cm^{-2})	HYPERMEC™ (1 mg cm^{-2})	Tokuyama A201	60	67	[73]

2 mL min^{-1} 0.25 M EG + 1 M KOH / 100 sccm O_2	PdNi/C (2 mg cm^{-2})	HYPERMEC™ (1 mg cm^{-2})	Tokuyama A201	60	27	[73]
2 mL min^{-1} 1 M EG + 1 M KOH / 100 sccm O_2	PdNi/C (2 mg cm^{-2})	HYPERMEC™ (1 mg cm^{-2})	Tokuyama A201	60	35	[73]
2 mL min^{-1} 3 M EG + 1 M KOH / 100 sccm O_2	PdNi/C (2 mg cm^{-2})	HYPERMEC™ (1 mg cm^{-2})	Tokuyama A201	60	22	[73]
2 mL min^{-1} 1 M EG + 5 M KOH / 100 sccm O_2	PdNi/C (2 mg cm^{-2})	HYPERMEC™ (1 mg cm^{-2})	Tokuyama A201	60	52	[73]
2 mL min^{-1} 1 M EG + 9 M KOH / 100 sccm O_2	PdNi/C (2 mg cm^{-2})	HYPERMEC™ (1 mg cm^{-2})	Tokuyama A201	60	60	[73]
2 mL min^{-1} 1 M EG + 7 M KOH / 100 sccm O_2	PdNi/C (1 mg cm^{-2})	HYPERMEC™ (1 mg cm^{-2})	KOH-doped PBI membrane	60	80	[74]
2 mL min^{-1} 0.5 M EG + 1 M KOH / 100 sccm O_2	PdNi/C (1 mg cm^{-2})	HYPERMEC™ (1 mg cm^{-2})	KOH-doped PBI membrane	60	28	[74]
2 mL min^{-1} 1 M EG + 1 M KOH / 100 sccm O_2	PdNi/C (1 mg cm^{-2})	HYPERMEC™ (1 mg cm^{-2})	KOH-doped PBI membrane	60	32	[74]
2 mL min^{-1} 2 M EG + 1 M KOH / 100 sccm O_2	PdNi/C (1 mg cm^{-2})	HYPERMEC™ (1 mg cm^{-2})	KOH-doped PBI membrane	60	23	[74]
2 mL min^{-1} 1 M EG + 3 M KOH / 100 sccm O_2	PdNi/C (1 mg cm^{-2})	HYPERMEC™ (1 mg cm^{-2})	KOH-doped PBI membrane	60	58	[74]
2 mL min^{-1} 1 M EG + 5 M KOH / 100 sccm O_2	PdNi/C (1 mg cm^{-2})	HYPERMEC™ (1 mg cm^{-2})	KOH-doped PBI membrane	60	72	[74]
2 mL min^{-1} 1 M EG + 9 M KOH / 100 sccm O_2	PdNi/C (1 mg cm^{-2})	HYPERMEC™ (1 mg cm^{-2})	KOH-doped PBI membrane	60	38	[74]
1 mL min^{-1} 1 M EG + 2 M KOH / 100 sccm humidified O_2 (RH=100%)	Pd-Cu/C	Pt black	Tokuyama A201	60	22	[85]
1 mL min^{-1} 1 M EG + 2 M KOH / 100 sccm humidified O_2 (RH=100%)	Pd/C	Pt black	Tokuyama A201	60	29	[85]
2 mL min^{-1} 5 wt% EG + 10 wt% KOH /200 mL min^{-1} air	Hypermec® 3020	Hypermec® 4014	Fumatech fumaPEM A alkaline membrane	70	~8.3	[16]
2 mL min^{-1} 5 wt% EG + 10 wt% KOH /200 mL min^{-1} air	Hypermec® 3020	Hypermec® 4014	Fumatech fumaPEM A alkaline membrane	80	~6.9	[16]

4 mL min^{-1} 2 M KOH + 5 wt % EG / 200 sccm humidified O_2 (RH=100%)	Pd-(Ni-Zn)/C (1 mg cm^{-2})	Fe-Co/C (1 mg cm^{-2})	Tokuyama A201	80	95	[61]
4 mL min^{-1} 2 M KOH + 5 wt % EG / 200 sccm humidified O_2 (RH=100%)	Pd/C (1 mg cm^{-2})	Fe-Co/C (1 mg cm^{-2})	Tokuyama A201	80	65	[61]
2 mL min^{-1} 1 M EG +7 M KOH / 100 sccm O_2	PdNi/C (1 mg cm^{-2})	HYPERMEC™ (1 mg cm^{-2})	KOH-doped PBI membrane	90	112	[74]
2 mL min^{-1} 1 M EG +7 M KOH / 100 sccm air	PdNi/C (1 mg cm^{-2})	HYPERMEC™ (1 mg cm^{-2})	KOH-doped PBI membrane	90	92	[74]

Table 2 Selected alkaline direct ethylene glycol fuel cell performance reported in the literature.

Graphical Abstract: This article reviews the past research on the development of alkaline direct ethylene glycol fuel cells, including the working principle, mechanisms and materials of the ethylene glycol oxidation, singe-cell performance, as well as innovative system designs.

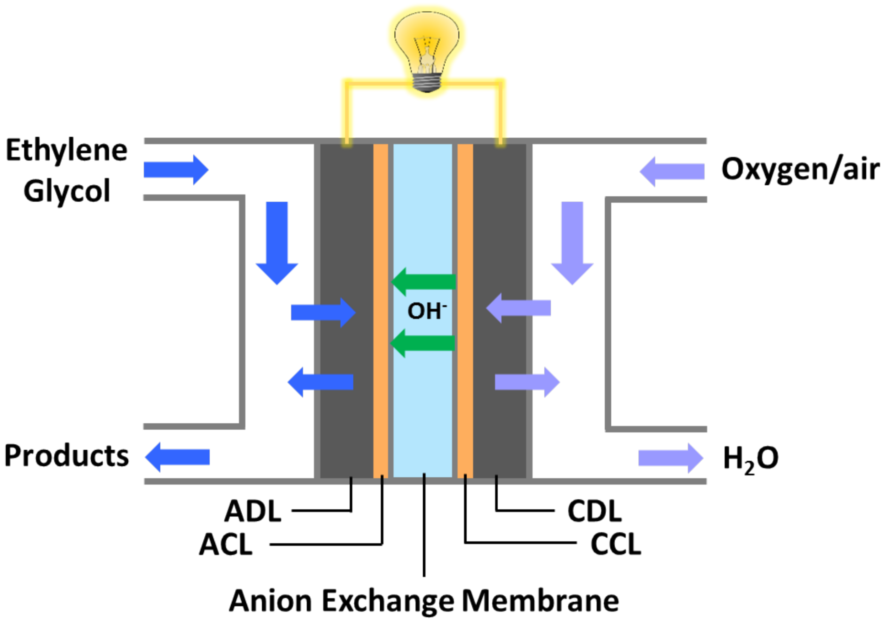

Highlights

- This article reviews past research on alkaline direct ethylene glycol fuel cells.
- Particular attention is paid to electrocatalytic oxidation of ethylene glycol.
- Single-cell performance is summarized and discussed.
- Innovative system designs and future perspectives are highlighted.